# Convergent epitope-specific T cell responses after SARS-CoV-2 infection and vaccination

Anastasia A. Minervina[1#], Mikhail V. Pogorelyy[1#], Allison M. Kirk[1], E. Kaitlynn Allen[1], Kim J. Allison[2], Chun-Yang Lin[1], David C. Brice[1], Xun Zhu[3], Kasi Vegesana[4], Gang Wu[3], Jeremy Chase Crawford[1], Stacey Schultz-Cherry[2], Jeremie H. Estepp[5], Maureen A. McGargill[1], the SJTRC Study Team✤, Joshua Wolf[2], Paul G. Thomas[1]

[1] Department of Immunology, St. Jude Children's Research Hospital, Memphis, TN USA
[2] Department of Infectious Diseases, St. Jude Children's Research Hospital, Memphis, TN USA
[3] Center for Applied Bioinformatics, St. Jude Children's Research Hospital, Memphis, TN USA
[4] Information Services, St. Jude Children's Research Hospital, Memphis, TN USA
[5] Department of Global Pediatric Medicine, St. Jude Children's Research Hospital, Memphis, TN USA

#Equal contribution

✤ Aditya Gaur, James Hoffman, Motomi Mori, Li Tang, Elaine Tuomanen, Richard Webby, Hana Hakim, Randall T. Hayden, Diego R. Hijano, Resha Bajracharya, Walid Awad, Lee-Ann Van de Velde, Brandi L Clark, Taylor L. Wilson, Robert C. Mettelman, Aisha Souquette, Ashley Castellaw, Ronald H. Dallas, Jason Hodges, Ashleigh Gowen, Jamie Russell-Bell, James Sparks, David E. Wittman, Thomas P. Fabrizio, Sean Cherry, Ericka Kirkpatrick Roubidoux, Valerie Cortez, Pamela Freiden, Nicholas Wohlgemuth, Kendall Whitt;

Correspondence to Joshua Wolf joshua.wolf@stjude.org and Paul Thomas paul.thomas@stjude.org

## Abstract

SARS-CoV-2 mRNA vaccines, including Pfizer/Biontech BNT162b2, were shown to be effective for COVID-19 prevention, eliciting both robust antibody responses in naive individuals and boosting pre-existing antibody levels in SARS-CoV-2-recovered individuals. However, the magnitude, repertoire, and phenotype of epitope-specific T cell responses to this vaccine, and the

effect of vaccination on pre-existing T cell memory in SARS-CoV-2 convalescent patients, are still poorly understood. Thus, in this study we compared epitope-specific T cells elicited after natural SARS-CoV-2 infection, and vaccination of both naive and recovered individuals. We collected peripheral blood mononuclear cells before and after BNT162b2 vaccination and used pools of 18 DNA-barcoded MHC-class I multimers, combined with scRNAseq and scTCRseq, to characterize T cell responses to several immunodominant epitopes, including a spike-derived epitope cross-reactive to common cold coronaviruses. Comparing responses after infection or vaccination, we found that T cells responding to spike-derived epitopes show similar magnitudes of response, memory phenotypes, TCR repertoire diversity, and αβTCR sequence motifs, demonstrating the potency of this vaccination platform. Importantly, in COVID-19-recovered individuals receiving the vaccine, pre-existing spike-specific memory cells showed both clonal expansion and a phenotypic shift towards more differentiated CCR7-CD45RA+ effector cells. In-depth analysis of T cell receptor repertoires demonstrates that both vaccination and infection elicit largely identical repertoires as measured by dominant TCR motifs and receptor breadth, indicating that BNT162b2 vaccination largely recapitulates T cell generation by infection for all critical parameters. Thus, BNT162b2 vaccination elicits potent spike-specific T cell responses in naive individuals and also triggers the recall T cell response in previously infected individuals, further boosting spike-specific responses but altering their differentiation state. Overall, our study demonstrates the potential of mRNA vaccines to induce, maintain, and shape T cell memory through vaccination and revaccination.

## Introduction

The ongoing COVID-19 pandemic led to the rapid development of novel types of antiviral vaccines, including the mRNA-based Pfizer/Biontech BNT162b2 regimen. Vaccination with BNT162b2 elicits both antibody and T cell responses (Sahin et al. 2020). However, the magnitude of T cell responses in naive individuals following infection or vaccination as well as the effect of vaccination on pre-existing memory cells remains controversial (Camara et al. 2021; Thimme et al. 2021; Painter et al. 2021), in part because the very nature of the T cell response complicates its unbiased quantification. While antibodies bind antigen directly, and thus can be measured and compared among donors using universal assays, T cells recognize antigen presented on the cell

surface by the Major Histocompatibility Complex (MHC), which is encoded by the most polymorphic genes in the human population (Robinson et al. 2019). Variability of peptide-MHC across and within donors makes measuring epitope-specific T cell responses challenging, and as a result studies often rely on bulk response (e.g., peptide stimulation) assays. Although peptide stimulation assays in principle can provide an estimate of the total CD8 response, they underestimate the frequency of epitope-specific T cells (Sahin et al. 2021). Staining with MHC-multimers loaded with individual peptides is an alternative approach, but it requires pre-selection of immunogenic peptides. Several immunodominant SARS-CoV-2 epitopes presented by common HLA alleles were discovered in the past year, permitting the tracking of epitope-specific T cell response in infected (Francis et al. 2021; Gangaev et al. 2021; Schreibing et al. 2021; Shomuradova et al. 2020; Kared et al. 2021; Saini et al. 2021; Ferretti et al. 2020; Nielsen et al. 2021; Peng, Yanchun et al. 2020; Rha et al. 2021; Sekine et al. 2020; Schulien et al. 2021; Habel et al. 2020; Nguyen et al. 2021) and vaccinated (Thimme et al. 2021; Sahin et al. 2021) individuals using MHC-multimers. Although at the peak of the infection response reports have described more than 10% of CD8+ T cells specific to a single SARS-CoV-2 epitope (Saini et al. 2021; Gangaev et al. 2021), a month after infection the frequency of most epitope-specific T cell populations is typically less than 1% (Ferretti et al. 2020; Peng, Yanchun et al. 2020; Kared et al. 2021; Rha et al. 2021). The rapid expansion and subsequent contraction of the T cell response occur in both infection (Thevarajan et al. 2020) and vaccination (Thimme et al. 2021), and careful choice of sampling timepoints is important to compare the magnitude of T cell responses in different donors. The diversity of T cell phenotypes adds another layer of complexity as effector and memory subpopulations differ in longevity, cytotoxic potential, and cytokine production.

Most vaccines are currently given in early childhood and are assessed by serological measures. When vaccine-induced T cell responses have been measured in humans or model systems, they frequently have reduced magnitude or narrower repertoires compared to natural infection (Cukalac et al. 2009; 2014; Oberle et al. 2016; Cornberg et al. 2006; Malherbe et al. 2008). Therefore, to directly compare the T cell response following infection or mRNA vaccination in naive and recovered COVID-19 individuals, we combined DNA-barcoded MHC-multimer staining (specific for spike and non-spike protein-derived epitopes) with scRNAseq and scTCRseq to profile epitope-specific T cell responses. We identified epitope-specific T cell responses of comparable

magnitude and phenotype following infection or naive vaccination, with further expansion of spike-specific T cells after convalescent vaccination. Longitudinal sampling of SARS-CoV-2 recovered donors before and after vaccination allowed us to observe clonal expansions and phenotype shifts among spike-specific memory T cells. Although the durability of immune protection provided by natural infection and primary vaccination remains unknown, our data suggest that mRNA vaccination in naive donors induces largely equivalent spike-specific T cell responses as infection, while revaccination with a spike-specific mRNA vaccine in recovered subjects can boost both T cell and antibody responses.

## Results

To investigate the ability of mRNA vaccines to trigger epitope-specific T cell responses as well as the effect of vaccination on memory T cells, we selected a cohort of 19 individuals from SJTRC, an ongoing prospective, longitudinal study of St. Jude Children's Research Hospital adult (≥18 years old) employees (Fig. 1A). Nine of these participants had never tested positive for COVID-19 during weekly PCR testing from the time SARS-CoV-2 reached the local area to time of sampling (naive, N1-N9), whereas 10 of the subjects were diagnosed as COVID-19 positive with a PCR test and recovered from mild disease (recovered, R1-R10) during the study period. Both the naive and recovered groups received two doses of the Pfizer-BioNTech BNT162b2 mRNA vaccine. Donors from each group were primarily chosen to ensure they were sampled at similar timepoints after the second dose of vaccine (R: 43±3.5; N: 46±3.5; Fig. S1A) and exhibited a similar distribution of HLA alleles of interest (Fig. S1B). PBMCs from recovered individuals were additionally obtained prior to the first vaccine dose ("post-infection" group, R1-R6), after the first dose (R7, R8, R10), or immediately subsequent to the second dose of vaccine (R9) (Fig. 1A). In concordance with previous reports (Goel et al. 2021; Krammer et al. 2021; Ebinger et al. 2021), we observed an anti-RBD (Fig. 1B) and anti-spike protein IgG (Fig. S2) boost after vaccination of recovered individuals. Two recovered individuals (R7 and R8) showed decreased RBD IgG post-second dose compared to the post-first dose sampling, though the decreases were minimal. Although it is generally accepted that recovered individuals do not benefit from the second dose of the vaccine (Wang et al. 2021; Mazzoni et al. 2021; Krammer et al. 2021; Goel et al. 2021; Ebinger et al. 2021; Camara et al. 2021), donor R10 clearly exhibited antibody boost due to the

second dose of BNT162b2. Overall, anti-RBD (Fig. 1B inset) and anti-spike IgG levels (Fig. S2) were similar between recovered and naive groups after vaccination. As expected, SARS-CoV-2-naive donors were negative for N-protein specific antibodies (Fig. S2), as only the S-protein is included in the vaccine. Thus, in both naive and recovered individuals, BNT162b2 vaccination induces high levels of anti-RBD and anti-spike IgG antibodies.

To evaluate epitope-specific CD8 T cell responses to mRNA vaccination, we selected 18 SARS CoV-2 epitopes (6 from the S protein and 12 from other proteins) that have been previously described by us or others, are likely to elicit a T cell response, and are presented on the common HLA alleles A*01:01, A*02:01, A*24:02, B*15:01 and B*44:02 (Fig. 1C, Supplementary Table 1) (Tarke et al. 2021; Kared et al. 2021; Snyder et al. 2020; Gangaev et al. 2021; Schulien et al. 2021; Nelde et al. 2021; Ferretti et al. 2020; Shomuradova et al. 2020; Peng, Yanchun et al. 2020; Sekine et al. 2020). In addition, four of the epitopes (A24_VYI, B15_NQK, B44_AEV and B44_VEN) were highly similar to orthologs from common cold coronaviruses (CCCoV), and the CCCoV variant MHC-dextramers were also included to test the cross-reactive potential of these epitopes.

PBMCs from each donor were stained with a panel of DNA-barcoded, fluorescently-labeled dextramers (Fig. 1A, Supplementary Table 2) that matched the donors' HLA alleles. For SARS-CoV-2-naive, vaccinated donors, these panels only included spike-derived MHC-dextramers. Epitope-specific T cells (CD3+CD8+dextramer+ cells) were isolated using FACS (Fig. S3) and then subjected to scRNAseq, scTCRseq, and CITEseq using the 10x Chromium platform. We obtained dextramer-positive CD8+ T cells from all naive, vaccinated donors and COVID-19 infected donors at convalescent timepoints and after vaccination, with varying frequencies. The overall frequency of dextramer-specific cells was quite low (0.23±0.05% of CD8+ T cells; range: 0.02-1% of CD8+ T cells), but matched expectations based on epitope-specific memory cells' frequencies observed months after the challenge in other studies (Ferretti et al. 2020; Peng, Yanchun et al. 2020; Kared et al. 2021; Rha et al. 2021). The absolute magnitude of epitope-specific T cell responses was similar across all groups (Fig. 1D) despite varying sources and episodes of antigen exposure.

Use of the DNA-barcoded dextramers allowed us to deconvolve the overall T cell response to 18 distinct epitope-specific responses. For each cell, we calculated the number of unique molecular identifiers (UMIs) per dextramer, and we considered a cell as dextramer-specific if more than 30% of the dextramer-derived UMIs corresponded to that dextramer's specific barcode. This resulted in non-overlapping dextramer-positive and -negative groups of cells for each dextramer (Fig. 2A, Fig. S4). To additionally test this threshold, we considered the dextramer assignment of individual cells among the 15 most abundant T cell clones (i.e., clone sizes ≥ 12 cells) defined by scTCRseq. Eleven of the most abundant clonotypes matched a single specificity across all cells (Fig. 2B), indicating that the dextramer specificity thresholds were generally robust. Interestingly, three of the most abundant TCR clonotypes were assigned to both B15-NQK_Q SARS-CoV-2 and B15-NQK_A CCCoV (HKU1/OC43) orthologs of the spike epitope, supporting our initial hypothesis for potential SARS-CoV-2/CCCoV epitope cross-reactivity. Indeed, the UMI counts for the dextramers with SARS-CoV-2 and CCCoV variants of the epitope correlated strongly (Fig. 2C), suggesting that the exact same cells can bind both versions of the epitope.

To further demonstrate that a single TCR can recognize both variants of B15-NQK, we made a Jurkat cell line expressing one of the potentially cross-reactive αβTCRs. This T cell line successfully recognized both CCCoV and SARS-CoV-2 variants of the peptide, as demonstrated by MHC-multimer staining (Fig. 2D) and peptide stimulation assays (Fig. S5). For 6 of 7 HLA-B*15 positive donors, we also measured antibody IgG levels against the spike protein of common cold betacoronaviruses HKU1 and OC43 prior to infection/vaccination. All of the donors except one had high titers of the antibodies (Fig. S6). Interestingly, the donor lacking antibodies to OC43/HKU1 also had the lowest T cell response to this epitope. These data indicate that SARS-CoV-2 may reactivate cross-reactive memory CD8+ T cells established during previous OC43/HKU1 infection.

Because barcoded dextramers allow us to simultaneously measure the response to multiple epitopes in the same sample on the single-cell level, we also utilized these data to compare the magnitude of the response to different epitopes. These analyses established that the most immunodominant epitopes include A01_TTD, A01_LTD, A02_YLQ and B15_NQK (Fig. 2E). Importantly, these epitopes not only elicited the strongest response, but also were found in all

HLA-matched samples. Although we observed responses to all other epitopes, they occurred at lower frequencies and only in a subset of HLA-matched donors. Epitopes A01_TTD, A24_NYN and A01_NTN are affected by mutations in SARS-CoV-2 variants of concern delta (P822L in the ORF1ab protein, L452R in the spike protein) and gamma (P80R in the N protein). However, models predicting peptide-MHC binding (NetMHCpan4.1b; (Reynisson et al. 2020)) suggest that these mutations do not impact the binding of the epitope to the restricting HLA allele, as both variants are predicted to be strong binders (Supplementary Table 3).

We next asked if we could identify signals corresponding to a T cell boost after the vaccination of SARS-CoV-2 recovered individuals. This can be difficult to resolve, as it requires accounting for clonal expansion of spike-specific T cells after vaccination and contraction of both spike- and non-spike-specific T cells following natural infection. The overall frequency of the spike-specific T cell response remained the same after vaccination, which is unsurprising given that the samples were obtained after memory formation. However, for the A02_YLQ spike epitope, we observed a trend towards a stronger T cell response in the context of vaccination (Fig. 2F). Although the overall frequency of epitope-specific cells may be the same before and after vaccination, or even decreasing after vaccination, the composition can shift due to the expansion of spike-specific clones (Fig. 2G, Fig. S7). Indeed, in 5 out of 6 donors, we observed an increase in the fraction of the spike-specific T cell response in comparison to the non-spike response after vaccination, indicating the recruitment of epitope-specific memory T cells among recovered individuals in the response to vaccination (Fig. 2H).

To understand if there are any differences in the phenotypes of epitope-specific T cells after natural infection, vaccination of naive, and vaccination of SARS-CoV-2 recovered individuals, we performed single cell gene expression (GEX) analysis. This analysis identified 8 distinct clusters of epitope-specific cells (Fig. 3A). According to the surface expression of conventional memory markers (CCR7 and CD45RA) measured by CITEseq (Fig. 3B) and other markers from scRNAseq (Fig 3C, Supplementary Table 4, Supplementary Table 5), the clusters were annotated as Effector Memory with expression of GZMK (EM-GZMK), EM with reexpression of CD45RA (EMRA), EM with exhaustion markers (EM-Ex), EM with high expression of mitochondrial genes (EM-Mito), Transitional memory (TM), naive/T stem cell-like memory, Cycling, and EM with GATA3.

Cells obtained either post-infection or post-vaccination were found across all gene expression clusters (Fig. S8, S9). Thus, natural infection, as well as vaccination, lead to the formation of potent T cell memory, including both highly cytotoxic populations and populations with expression of common markers of durable cellular memory, including TCF7, IL7R, and CCR7 (Fig. 3C).

To determine if a recall response during vaccination affects the phenotypes of T cells, we compared the GEX cluster distribution of recovered donors post-infection and post-vaccination. Epitope-specific T cells were present in all clusters before and after vaccination, independent of their specificity (Fig. 3D). However, we observed a significant post-vaccination shift towards a more highly differentiated effector phenotype (EMRA) of spike-specific cells, but not for non-spike-specific cells, suggesting that this shift was due to the involvement of spike-specific memory T cells in the recall response to vaccination in convalescent donors (Fig. 3E, ($p=0.007$, one-tailed Wilcoxon rank-sum test).

Recent publications have linked T cell exhaustion to more severe COVID-19 (Kusnadi et al. 2021; Zheng et al. 2020; Diao et al. 2020). Our epitope-specific data similarly included a cluster with high expression of classical exhaustion markers, including CTLA-4, PD-1, TOX, and TIGIT (Cluster 2, EM-Ex, Fig. 3C). Interestingly, this cluster was present only in a fraction of donors, but was present across all conditions: naive donor after vaccination (donors N3, N6, N9), post-infection (R1, R6), post-first dose in recovered donors (R7), and post-second dose in recovered donors (R4, R9). Thus, the appearance of this cluster was not connected to disease severity or the nature of the antigenic stimulus (vaccine or virus). In concordance with previous reports (Schreibing et al. 2021; Kusnadi et al. 2021), this cluster was composed of highly expanded clones (Fig. S10), with more than 87% of the cluster repertoire occupied by just 10 clones (Fig. 3F). We also observed that a cluster of exhausted cells was in close proximity in UMAP-space with a cluster of cycling cells with high expression of MKI67 and TUBB (Fig. 3A, Fig. 3C), indicating a possible connection between these two phenotypic states. Indeed, the number of cells in an exhausted cluster within a patient strongly correlated with the number of cells in the cluster of cycling cells (Fig. 3G). Thus, the presence of the exhausted cluster is connected to both clonal expansion and cell proliferation, suggesting that donors who have such cells are still in the active rather than memory state of immune response. If the “exhausted” cluster is indeed the feature of an active

249 immune response state, it must be transient. To test this, we looked at the distribution of cells
250 among clusters at two available timepoints for recovered individuals (average time between
251 timepoints was 81 days, range 47-121). Almost all cells from this exhausted cluster were absent
252 from the epitope-specific pool of memory T cells at the later timepoint (Fig. 3H). This was
253 observed for both spike and non-spike-specific cells, indicating that the vaccine does not impact
254 the survival of these "exhausted" cells.
255
256 The majority of the clonotypes in the exhausted cluster are highly expanded and are present among
257 other clusters of memory T cells. While the majority of the "exhausted" T cells apparently die, the
258 clonotype lineage and thus the specificity of T cell response is preserved in the EM and EMRA
259 compartments (Fig. 3I). Importantly, the overall TCRβ repertoire diversity (represented by
260 normalised Shannon entropy) is comparable between vaccinated naive donors, post-infection
261 donors, and the post-infection/post-vaccination donors (Fig 3J), suggesting that a diverse repertoire
262 of T cells persists in the memory compartment regardless of antigenic history. This is distinct from
263 other models comparing vaccination to infection (Cukalac et al. 2009; Malherbe et al. 2008).
264
265 We and others have previously shown that T cells recognizing the same epitopes frequently have
266 highly similar T cell receptor sequences (Glanville et al. 2017; Dash et al. 2017). In Fig. 4A, we
267 plot a similarity network of paired unique αβTCR sequences from our data (Supplementary table
268 6), using a threshold on the TCRdist (Dash et al. 2017) similarity measure to identify highly similar
269 clonotypes. The clusters of similar sequences almost exclusively consist of TCRs with the same
270 epitope specificity and feature biases in V-segment usage (Fig. S11, S12) and strong preference
271 for certain amino acid residues at certain positions of CDR3 region (Fig. 4B). Importantly, the
272 same motifs in spike-specific TCRs were shared between donors who recovered from natural
273 infection and immunologically naive donors after immunization (Fig. 4C). Furthermore, the most
274 prevalent TCR sequence motif specific to A02_YLQ was present across all HLA-matched samples
275 studied. This suggests that epitope recognition is achieved by the same TCR-pMHC molecular
276 interactions, and thus one could expect similar specificity to potential epitope variants for memory
277 T cells elicited by vaccination or natural infection.
278

## Discussion

Vaccination was shown to be effective in preventing COVID-19, but durability of protection is yet to be determined. It is critical to understand if pre-existing SARS-CoV-2 immunity could be successfully boosted through vaccination. We show that the Pfizer/Biontech BNT162b2 vaccine boosts both antibody levels and T cells specific for SARS-CoV-2 spike protein in individuals with pre-existing immunity for natural infection. We also show that there is no profound difference in frequency, phenotype, or TCR motifs in memory T cells generated by natural infection and vaccination. Taken together, this suggests that mRNA vaccines would be also effective for boosting of pre-existing vaccine-induced immunity during revaccination. The direct comparison between infection- and vaccine-elicited T cell responses has not been well-studied previously in humans as most vaccines are given in very young children. The success of those vaccines also limits the population that acquire natural infection as a comparator group.

We also discovered T cells cross-reactive for SARS-CoV-2 and common cold coronavirus variants of an HLA*B15-restricted immunodominant epitope. The possibility of this cross-reactivity was hypothesized in (Minervina et al. 2021), where the clonotypes with this TCR motif were the most expanded in an HLA-B*15 positive donor. Francis et al. recently described HLA-B*07_SPR, another epitope from N-protein, as being cross-reactive with HKU1 and OC43 common-cold coronaviruses. The extent of protection in HLA-B*15 and HLA-B*07 positive donors recently infected with common cold coronaviruses is yet to be determined, but a high frequency of cross-reactive CD8 T cells may be a correlate of protection.

Using longitudinal sampling, we show that certain T cell populations, including differentiated effector cells with exhaustion markers or actively proliferating T cells, are transient and not found in the same donor at later timepoints. Expanded clones contributing to these transient clusters persist in other clusters with long lived memory phenotype. This result agrees with the functional experiment from Gangaev et al. who showed that a fraction of epitope specific T cells sampled close to acute infection timepoints are dysfunctional, but restore IFNgamma/TNFa production further into convalescence. The exhausted T cell phenotype was previously linked to more severe disease (Kusnadi et al. 2021; Zheng et al. 2020; Diao et al. 2020), but our data suggests that time

since immune stimulus (either infection or vaccination) could also explain the presence of these exhausted effectors. Given that many severe patients may have extended viral replication dynamics, their sampling may occur closer to recent antigen exposure. This does not preclude the accumulation of exhausted T cells as contributing to severe disease phenotypes, but it also might merely be a correlate of extended antigen exposure. Further, the presence of this exhausted phenotype in subjects with all forms of antigen exposure indicates that the presence of these cells is not sufficient to cause significant pathology.

An important limitation of our study is that we could not compare the effect of one vs two doses of mRNA vaccine in individuals with pre-existing immunity. It has been suggested in multiple studies that a second vaccine dose in individuals with pre-existing immunity does not further increase antibody levels from the first dose (Wang et al. 2021; Mazzoni et al. 2021; Krammer et al. 2021; Goel et al. 2021; Ebinger et al. 2021; Camara et al. 2021), but the effect on T cells remains to be studied. We found an increase in the fraction of EMRA T cells in fully vaccinated subjects with pre-existing immunity. Whether or not this increase is associated with more (or less) durable and efficient protection is not clear. Longer term follow-up studies of the durability of memory in vaccine-only, infection-only, and vaccinated after infection groups should closely monitor the phenotype of antigen-specific T cell responses.

Precise measurement of epitope-specific T cell and B cell responses is crucial for defining the correlates of SARS-CoV-2 protection, which will inform vaccination strategies to prevent pandemic recurrence as additional SARS-CoV-2 variants emerge. The striking similarity between the phenotypes and constituent repertoires of epitope-specific CD8 T cell responses following infection, vaccination, or infection followed by vaccination, indicate that mRNA vaccines are capable of inducing equivalent memory as an infection episode and further expanding these responses if previously established. These data further suggest that booster shots, if needed to address antibody-escape, will not substantially alter the repertoires of established anti-spike T cell memory. These data are a stark contrast to annual, non-adjuvanted split influenza vaccines, where repeated vaccination has raised some concerns of immune imprinting, tolerance, and reduced vaccine efficacy (Petrie and Monto 2017). While longer term comparative studies between

vaccinated and infected individuals are necessary, our results establish BN162b2 vaccination as a potent inducer of SARS-CoV-2 specific CD8 T cells with a profile equivalent to natural infection.

## Methods

### Human cohort

The St. Jude Tracking of Viral and Host Factors Associated with COVID-19 study (SJTRC, NCT04362995) is a prospective, longitudinal cohort study of St. Jude Children's Research Hospital adult (≥18 years old) employees. The St. Jude Institutional Review Board approved the study. Participants provided written informed consent prior to enrollment and then completed regular questionnaires about demographics, medical history, treatment, and symptoms if positively diagnosed by PCR with SARS-CoV-2. Study data are collected and managed using REDCap electronic data capture tools hosted at St. Jude (Harris et al. 2009; 2019). Participants were screened for SARS-CoV-2 infection by PCR approximately weekly when on St. Jude campus. For this study, we selected a cohort of 19 individuals, nine of which had never tested positive for COVID-19 (naive, N1-N9), and 10 of which were diagnosed as COVID-19 positive with a PCR test and recovered from mild disease (recovered, R1-R10) during the study period. All individuals in this study received two doses of the Pfizer-BioNTech BNT162b2 mRNA vaccine and, most importantly, were sampled at similar time points after their vaccine regimen was complete (Recovered: 43±3.5; Naive: 46±3.5; Fig. S1A). These individuals also expressed a similar distribution of HLA allele of interest (A01:01, A02:01, A24:02, B15:01, B44:02; Fig. S1B). Finally, the individuals chosen for each group were of similar ages (Recovered: 44.5±4.9 years; Naive: 42.7±3.5 years). For this study, we utilized the convalescent blood draw for SARS-CoV-2 infected individuals (3-8 weeks post diagnosis) and the post-vaccination samples for both SARS-CoV-2 convalescent and naive individuals (3-8 weeks after completion of the vaccine series). Blood samples were collected in 8 mL CPT tubes and separated within 24 hours of collection into cellular and plasma components and aliquoted and frozen for future analysis. Human cohort metadata can be found in the Supplementary Table 2.

**HLA typing**

High quality DNA was extracted from whole blood aliquots from each participant using the Zymo Quick-DNA 96 Plus Kit (Qiagen). DNA was quantified on the Nanodrop. HLA typing of each participant was performed using the AllType NGS 11-Loci Amplification Kit (One Lambda; Lot 013) according to manufacturer's instructions. Briefly, 50 ng DNA was amplified using the AllType NGS 11-Loci amplification primers, and the amplified product was cleaned and quantified on the Qubit 4.0 (Invitrogen). Library preparation of purified amplicons was carried out as described in the protocol, and the AllType NGS Index Flex Kit (Lot 011) was used for barcoding and secondary amplification. Purified, barcoded libraries were quantified using the Qubit DNA HS kit (Invitrogen) and pooled according to the One Lambda Library Pooling table. Pools of up to 48 libraries were then purified and then quantified on the TapeStation D5000 (Agilent) before sequencing on a full MiSeq lane at 150x150bp following manufacturer's sequencing specifications. HLA types were called using the TypeStream Visual Software from One Lambda. HLA typing results can be found in the Supplementary Table 2.

**Variant of concern mutation analysis**

We used the WHO definition of variant of concern and variant of interest updated July 6, 2021. A mutation was included in the analysis if it appears in at least 10% of the GISAID isolates with the same Pango lineage (Rambaut et al. 2020). To analyze the predicted binding of variant and wild type peptides we used NetMHCpan 4.1b (Reynisson et al. 2020). Results of this analysis are in Supplementary Table 3.

**Dextramer generation and cell staining**

Peptides with >95% purity were ordered from Genscript and diluted in DMSO to 1 mM. pMHC monomers (500 nM) were generated with easYmer HLA class I (A*01:01, A*02:01, A*24:02, B*15:01, B*44:02) kits (Immunaware) according to the manufacturer's protocol. To generate DNA-barcoded MHC-dextramers we used Klickmer technology (dCODE Klickmer, Immudex). 16.2 µL of HLA monomer (500 nM) were mixed with 2 µL barcoded dCODE-PE-dextramer to achieve an average occupancy of 15 and incubated for at least 1 hour on ice prior to use. Individual dextramer cocktails were prepared immediately before staining (Supplementary Table 2). Each cocktail had 1.5 µL of each HLA-compatible barcoded MHC-dextramer-PE and 0.15 µL 100 µM

biotin per dextramer pre-mixed to block free binding sites. Samples were divided into 3 batches, and timepoints from the same donor were always processed simultaneously. Donor PBMCs were thawed and resuspended in 50 µL FACS buffer (PBS, 0.5% BSA, 2 mM EDTA). Cells were stained with 5 µL Fc-block (Human TruStain FcX, Biolegend 422302) and a cocktail of dextramers for 15 minutes on ice. After this a cocktail of fluorescently-labeled surface antibodies (2 µL of each: Ghost Dye Violet 510 Viability Dye, Tonbo Biosciences 13-0870-T100; anti-human CD3 FITC-conjugated (Biolegend 300406, clone UCHT1), anti-human CD8 BV711-conjugated (Biolegend, 344734, clone SK1)) and TotalSeq-C antibodies (1 µL anti-human CCR7 (Biolegend 353251), 1 µL anti-human CD45RA (Biolegend 304163)) and 2 µL of TotalSeq-C anti-human Hashtag antibodies 1-10 (Biolegend 394661, 394663, 394665, 394667, 394669, 394671, 394673, 394675, 394677, 394679) were added. Samples were incubated for 30 minutes on ice. Single, Live, CD3-positive, CD8-positive, dextramer-positive cells were sorted into RPMI (Gibco) containing 10% FBS and 1% penicillin/streptomycin. Sorted cells were immediately loaded into a 10x reaction. Chromium Next GEM Single Cell 5' kits version 2 (10x Genomics PN: 1000265, 1000286, 1000250, 1000215, 1000252 1000190, 1000080) were used to generate GEX, VDJ and Cite-Seq libraries according to the manufacturer's protocol. Libraries were sequenced on Illumina NovaSeq at 26x90bp read length.

**Single cell RNAseq data analysis**

Raw data was processed with Cell Ranger version 6.0.0 (10X Genomics). Three batches were subsequently combined using the aggregate function with default parameters. Resulting GEX matrices were analysed with the Seurat R package version 3.2.3 (Stuart et al. 2019). Following standard quality control filtering, we discarded low quality cells (nFeatures<200 or over 5000, MT%>10%) and eliminated the effects of cell cycle heterogeneity using the CellCycleScoring and ScaleData functions. Next, we identified 2000 variable gene features. Importantly, we discarded TCR/Ig genes from variable features, so that the gene expression clustering would be unaffected by T cell clonotype distributions. Next, we removed all non-CD8 cells from the data as well as cells labeled with antibody hashtag #1 (Biolegend 394661) in batch 3, which were used solely as carrier cells for the 10X reaction. Differentially expressed genes between clusters were found using the Seurat FindAllMarkers function with default parameters, and resolution parameter set to 0.5. Differentially expressed genes for 8 resulting clusters can be found in Supplementary Table 4. R

scripts for the final Seurat object generation can be found on GitHub (https://github.com/pogorely/COVID_vax_CD8).

**Donor and epitope assignment using feature barcodes**

Cells were processed in 3 batches (each batch making a separate 10x Chromium reaction). In each batch, each PBMC sample was uniquely labeled with a DNA-barcoded hashing antibody (TotalSeq-C anti-human Hashtag antibodies 1-10, Biolegend). We attributed a cell to a certain donor if more than 50% of UMIs derived from hashing antibodies were from the hashtag corresponding to that donor. Cells specific to certain dextramers were called similarly: we required more than 30% of dextramer-derived UMIs to contain a dextramer-specific barcode, and if multiple dextramers passed this threshold the cell was considered specific to both. If the most abundant dextramer barcode per cell was ≤ 3 UMIs, we did not assign any epitope specificity to it. TCRα and TCRβ sequences were assembled from aggregated VDJ-enriched libraries using CellRanger (v. 6.0.0) vdj pipeline. For each cell we assigned the TCRβ and TCRα chain with the largest UMI count. The R script performing feature barcode deconvolution, GEX and TCR join is available on Github (https://github.com/pogorely/COVID_vax_CD8) as well as the resulting Supplementary Table 5.

**TCR repertoire analysis**

A T cell clone was defined as a group of cells from the same donor which have the same nucleotide sequences of both CDR3α and CDR3β (see Supplementary Table 6 for unique T cell clones). To measure the distance between TCR α/β clonotypes and plot logos for dominant motifs we used the TCRdist algorithm implementation and plotting functions from *conga* python package (Schattgen et al. 2020). TCRβ repertoire diversity calculation was performed using normalized Shannon entropy $-(\sum_{i=1}^{n} p_i log_2(p_i))/log_2(n)$, where $n$ is a total number of unique TCRβ clonotypes, and $pi$ is a frequency of $i$-$th$ TCRβ clonotype (defined as the fraction of cells with this TCRβ of all cells in a sample with defined TCRβ). Similarity network analysis and visualization were performed with the *igraph* R package (Csardi and Nepusz 2006) and *gephi* software (Jacomy et al. 2014).

**Artificial antigen-presenting cells (aAPCs)**

A gBlock gene fragment encoding full-length HLA-B*15:01 was synthesized by Genscript and cloned into the pLVX-EF1α-IRES-Puro lentiviral expression vector (Clontech). Lentivirus was generated by transfecting 293T packaging cell line (American Type Culture Collection (ATCC) CRL-3216) with the pLVX lentiviral vector containing the HLA-B*15:01 insert, psPAX2 packaging plasmid (Addgene plasmid #12260), and pMD2.G envelope plasmid (Addgene plasmid #12259). Viral supernatant was harvested and filtered 24- and 48-hours post-transfection, then concentrated using Lenti-X Concentrator (Clontech). K562 cells (ATCC CCL-243) were transduced, then antibiotic selected for one week using 2 μg/mL puromycin in Iscove's Modified Dulbecco's Medium (IMDM; Gibco) containing 10% FBS and 1% penicillin/streptomycin. Surface expression of HLA was confirmed via flow cytometry using antibodies against HLA-A, B, C (PE-conjugated, Biolegend 311406, clone W6/32).

**TCR-expressing Jurkat 76.7 cells**

TCRα (TRAV21, CAVHSSGTYKYIF, TRAJ40) and TCRβ (TRBV7-2, CASSLEDTNYGYTF, TRBJ1-2) chains matching both the biggest B15_NQK-specific motif on Fig 4B and prediction from (Minervina et al. 2021) were selected for Jurkat cell line generation. TCRα and TCRβ chains for the selected B15_NQK-specific TCR were modified to use murine constant regions (murine TRAC*01 and murine TRBC2*01). A gBlock gene fragment was synthesized by Genscript to encode the modified TCRα chain, the modified TCRβ chain, and mCherry, with all three genes linked together by 2A sites. This sequence was cloned into the pLVX-EF1α-IRES-Puro lentiviral expression vector (Clontech). Lentivirus was generated by transfecting 293T packaging cell line (ATCC CRL-3216) with the pLVX lentiviral vector containing the TCR-mCherry insert, psPAX2 packaging plasmid (Addgene plasmid #12260), and pMD2.G envelope plasmid (Addgene plasmid #12259). Viral supernatant was harvested and filtered 24- and 48-hours post-transfection, then concentrated using Lenti-X Concentrator (Clontech). Jurkat 76.7 cells (a gift from Wouter Scheper; variant of TCR-null Jurkat 76.7 cells that expresses human CD8 and an NFAT-GFP reporter) were transduced, then antibiotic selected for 1 week using 1 μg/mL puromycin in RPMI (Gibco) containing 10% FBS and 1% penicillin/streptomycin. Transduction was confirmed by expression of mCherry, and surface TCR expression was confirmed via flow cytometry using

antibodies against mouse TCRβ constant region (PE-conjugated, Biolegend 109208, clone H57-597) and human CD3 (Brilliant Violet 785-conjugated, Biolegend 344842, clone SK7).

**Intracellular cytokine staining functional assay**

Jurkat 76.7 cells expressing the B15_NQK-specific TCR ($2.5x10^5$) were cocultured with HLA-B*15:01 aAPCs ($2.5x10^5$) pulsed with 1 μM of either NQKLIANAF peptide from HKU1/OC43 common cold coronaviruses or NQKLIANQF peptide from SARS-CoV2, 1 μg/mL each of anti-human CD28 (BD Biosciences 555725) and CD49d (BD Biosciences 555501), brefeldin A (GolgiPlug, 1 μL/mL; BD Biosciences 555029), and monensin (GolgiStop, 0.67 μL/mL; BD Biosciences 554724). An unstimulated (CD28, CD49d, brefeldin A, monensin) and positive control (brefeldin A, monensin, 1X Cell Stimulation Cocktail, PMA/ionomycin; eBioscience 00-4970-93) were included in each assay. Cells were incubated for 6 hours (37 $^oC$, 5% $CO_2$). Following the 6-hour incubation, cells were washed twice with FACS buffer (PBS, 2% FBS, 1 mM EDTA), then blocked using human Fc-block (BD Biosciences 564220). Cells were then stained with 1 μL Ghost Dye Violet 510 Viability Dye (Tonbo Biosciences 13-0870-T100) and a cocktail of surface antibodies: 1 μL each of anti-human CD8 (Brilliant Violet 785-conjugated, Biolegend 344740, clone SK1), anti-human CD3 (Brilliant Violet 421-conjugated, Biolegend 344834, clone SK7), and anti-mouse TCRβ chain (PE-conjugated (Biolegend 109208) or APC/Fire750-conjugated (Biolegend 109246), clone H57-597). Cells were then washed twice with FACS buffer, then fixed and permeabilized using the Cytofix/Cytoperm Fixation/Permeabilization kit (BD Biosciences) according to the manufacturer's instructions. Following fixation and permeabilization, cells were washed twice with 1X Perm/Wash buffer and stained with a cocktail of intracellular antibodies: 1.25 μL of anti-human IFNγ (Alexa Fluor 647-conjugated, Biolegend 502516, clone 4S.B3) and 1 μL anti-human CD69 (PerCP-eFluor710-conjugated, eBioscience 46-0699-42, clone FN50). Cells were then washed twice with 1X Perm/Wash buffer and analyzed by flow cytometry on a custom-configured BD Fortessa using FACSDiva software (Becton Dickinson). Flow cytometry data were analyzed using FlowJo software (TreeStar). Responsiveness to peptide stimulation was determined by measuring frequency of NFAT-GFP, IFNγ, and CD69 expression.

**Tetramer generation and Jurkat Cell line staining**

Biotinylated HLA-B*15-monomers loaded with NQKLIANQF (SARS-CoV-2) and NQKLIANAF (CCCoV) versions of the peptide were tetramerised using TotalSeq-C-0951-PE-Streptavidin (Biolegend 405261) and TotalSeq-C-0956-APC-Streptavidin (Biolegend 405283). 60 µL of HLA-monomers were mixed with 1 µL of PE-conjugated (for B15_NQKLIANQF) and APC-conjugated for (B15_NQKLIANAF) streptavidin reagents and incubated for 1 hour in the dark on ice. Jurkat 76.7 cells expressing the potentially cross-reactive TCR were stained with 1 µL Ghost Dye Violet 510 Viability Dye (Tonbo Biosciences 13-0870-T100) and 5 µL of each MHC-tetramer. Flow cytometry data were analyzed using FlowJo software (TreeStar). Cross-reactivity of the Jurkat 76.7 T cell line was determined by co-staining of the live cells with PE and APC-labeled MHC-tetramers.

**Recombinant SARS-CoV-2 proteins and ELISA**

Expression plasmids for the nucleocapsid (N) protein, spike protein, and the spike receptor binding domain (RBD) from the Wuhan-Hu-1 isolate were obtained from Florian Krammer. Proteins were transfected into Expi293F cells using a ExpiFectamine 293 transfection kit (Thermo Fisher Scientific) as previously described (Amanat et al. 2020). Supernatants from transfected cells were harvested and purified with a Ni-NTA column.

For hCoV and SARS-CoV-2 antibody detection, 384-well microtiter plates were coated overnight at 4 °C, with recombinant proteins diluted in PBS. Optimal concentrations for each protein and isotype were empirically determined to optimize sensitivity and specificity. SARS-CoV-2 spike RBD was coated at 2 µg/mL in PBS. Full-length spike was coated at 2 µg/mL for IgG. N protein was coated at 1 µg/mL. The spike proteins of hCoV-229E (Sino Biological, 40605-V08B), hCoV-NL63 (Sino Biological, 40604-V08B), hCoV-HKU1 (Sino Biological, 40606-V08B), or hCoV-OC43 (Sino Biological, 40607-V08B) were coated at 1 µg/mL for IgG detection. For all ELISAs, plates were washed the next day three times with 0.1% PBS-T (0.1% Tween-20) and blocked with 3% Omniblok™ non-fat milk (AmericanBio; AB10109-01000) in PBS-T for one hour. Plates were then washed, and incubated with plasma samples diluted 1:50 in 1% milk in PBS-T for 90 minutes at room temperature. Prior to dilution, plasma samples were incubated at 56 °C for 15 minutes. ELISA plates were washed and incubated for 30 minutes at room temperature with anti-human secondary antibodies diluted in 1% milk in PBS-T: anti-IgG (1:10,000; Invitrogen, A18805). The

plates were washed and incubated at room temperature with OPD (Sigma-Alrich, P8287) for 10 minutes (for hCoV ELISAs) or SIGMAFAST OPD (Sigma-Alrich; P9187) for 8 minutes (for SARS-CoV-2 ELISAs) and absorbances were measured at 490 nm on a microplate reader. To ensure the specificity of this assay, we first screened samples from a prior study that included young children to identify samples to serve as negative controls. In addition, as a control for plate-to-plate variability, we selected two positive samples from the SJTRC cohort that were tested on each plate and used to calculate the percent ratio, which is the OD of each sample relative to the OD of the control samples. Samples with a percent ratio greater than three times the average of the negative controls were considered positive for the hCoV and two times the average of the negative controls for the SARS-CoV-2 antigens. Antibody levels for each donor can be found in the Supplementary Table 2.

**Statistical analysis**

Statistical analysis was performed in R version 4.0.3. Wilcoxon signed-rank test was used to compare paired pre-vaccination and post-vaccination samples, Wilcoxon rank-sum test was used to compare unpaired samples between study groups.

**Data and code availability**

Code required to reproduce source data for figures is available on GitHub: https://github.com/pogorely/COVID_vax_CD8. All data produced in the study is available as supplementary files. Raw sequencing data was deposited to Short Read Archive acc. PRJNA744851.

**Acknowledgements**

We thank all the donors who volunteered for the SJTRC study, Phil Bradley and Stefan Schattgen for their consultations on TCRdist and conga algorithms, Greig Lennon from St. Jude Immunology flow core for his help with FACS, and Hartwell Center for high-throughput sequencing. This work was funded by ALSAC at St. Jude, the Center for Influenza Vaccine Research for High-Risk Populations (CIVR-HRP) contract number 75N93019C00052 (S.S-C, P.G.T), the St. Jude Center of Excellence for Influenza Research and Surveillance (S.S-C, M.A.M, P.G.T),

HHSN272201400006C, 3U01AI144616-02S1 (P.G.T, M.A.M, S.S-C), and R01AI136514 (P.G.T).

## Author Contributions

Conceptualization: A.A.M, M.V.P, E.K.A, J.C.C. and P.G.T. Formal analysis: A.A.M, M.V.P, A.M.K, J.C.C, M.A.M, J.W, J.H.E, X.Z, K.V, G.W. Investigation: A.A.M., M.V.P, A.M.K, M.A.M, J.W, J.E., C-Y.L, D.B. Methods development: A.A.M, M.V.P, A.M.K, C-Y.L, S.S-C, M.A.M. Resources: S.S-C, M.A.M, P.T, J.H.E., J.W. Data and sample curation: J.W, J.H.E, E.K.A, K.J.A, SJTRC Study Team. Writing, original draft: A.A.M. and M.V.P. Writing, review, and editing: A.A.M, M.V.P, A.M.K, E.K.A, J.C.C, J.W, M.A.M, P.G.T. Visualization: A.A.M. Supervision: P.G.T. Funding Acquisition: P.G.T.

## Competing interests

P.G.T has consulted or received honorarium and travel support from Illumina and 10X. P.G.T. serves on the Scientific Advisory Board of Immunoscape and Cytoagents.

## Supplementary information

**Supplementary Table 1.** SARS-CoV-2 derived CD8+ epitopes used for MHC-multimer generation.

**Supplementary Table 2**. Study participants metadata.

**Supplementary Table 3.** Mutations in studied epitopes from SARS-CoV-2 variants.

**Supplementary Table 4.** Differentially expressed genes for GEX clusters of epitope-specific CD8+ T cells.

**Supplementary Table 5.** Epitope-specific CD8+ T cells GEX clusters, TCR and epitope specificity.

**Supplementary Table 6.** Unique epitope-specific CD8+ αβTCR clonotypes.

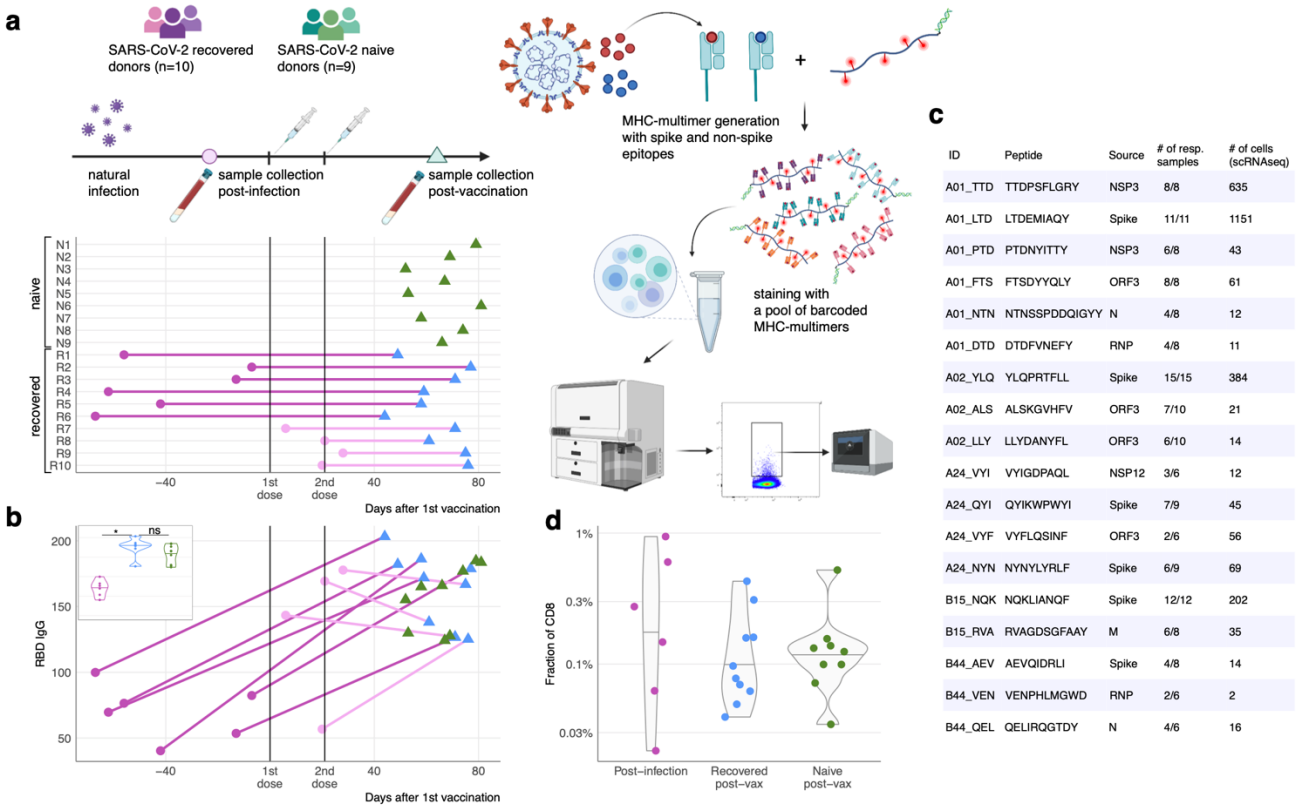


| ID | Peptide | Source | # of resp. samples | # of cells (scRNAseq) |
|---|---|---|---|---|
| A01_TTD | TTDPSFLGRY | NSP3 | 8/8 | 635 |
| A01_LTD | LTDEMIAQY | Spike | 11/11 | 1151 |
| A01_PTD | PTDNYITTY | NSP3 | 6/8 | 43 |
| A01_FTS | FTSDYYQLY | ORF3 | 8/8 | 61 |
| A01_NTN | NTNSSPDDQIGYY | N | 4/8 | 12 |
| A01_DTD | DTDFVNEFY | RNP | 4/8 | 11 |
| A02_YLQ | YLQPRTFLL | Spike | 15/15 | 384 |
| A02_ALS | ALSKGVHFV | ORF3 | 7/10 | 21 |
| A02_LLY | LLYDANYFL | ORF3 | 6/10 | 14 |
| A24_VYI | VYIGDPAQL | NSP12 | 3/6 | 12 |
| A24_QYI | QYIKWPWYI | Spike | 7/9 | 45 |
| A24_VYF | VYFLQSINF | ORF3 | 2/6 | 56 |
| A24_NYN | NYNYLYRLF | Spike | 6/9 | 69 |
| B15_NQK | NQKLIANQF | Spike | 12/12 | 202 |
| B15_RVA | RVAGDSGFAAY | M | 6/8 | 35 |
| B44_AEV | AEVQIDRLI | Spike | 4/8 | 14 |
| B44_VEN | VENPHLMGWD | RNP | 2/6 | 2 |
| B44_QEL | QELIRQGTDY | N | 4/6 | 16 |

**Fig 1. Measuring CD8+ T cell epitope-specific responses in SARS-CoV-2 naive and recovered individuals after mRNA vaccination. a. Study design.** Left: Peripheral blood samples SARS-CoV-2 naive donors (n=9) and SARS-CoV-2 recovered donors (n=10) were collected after 2 doses of Pfizer/BioNtech vaccine. For SARS-CoV-2 recovered donors, we collected another sample at a previous timepoint before (purple, "post-infection") or after vaccination (pink, "post-vax"). Time of blood sampling for each donor is shown relative to the first dose of vaccine. Right: Selected spike and non-spike SARS-CoV-2 T cell epitopes were loaded on recombinant biotinylated MHC-monomers. Resulting peptide-MHC complexes were polymerized using fluorescently-labeled and DNA-barcoded dextran backbones. Next, we stained PBMC samples with pools of MHC-multimers, isolated bound cells using FACS, and performed scRNAseq, scTCRseq, and CITEseq using the 10X Genomics platform. **b. Anti-RBD IgG antibody levels in SARS-CoV-2 recovered individuals increase after immunization with Pfizer-BioNTech BNT162b2 (p=0.016, Wilcoxon signed-rank test).** Inset: after two doses of vaccine anti-RBD IgG levels are the same for SARS-CoV-2 naive donors (green) and SARS-CoV-2 recovered donors (blue) (p=0.18, Wilcoxon rank-sum test) and both are larger than post-infection levels in SARS-CoV-2 recovered donors (purple). **c. List of SARS-CoV-2 epitopes used in this study.** Table shows peptide sequences, source proteins, and summary statistics for resulting epitope-specific responses (number of HLA-matched samples with a response and number of epitope-specific cells recovered from scRNAseq). **d. Total frequency of MHC-dextramer-positive cells is similar in SARS-CoV-2 recovered individuals post-infection (purple) and post-vaccination (blue), and in SARS-CoV-2 naive donors post-vaccination (green).** Percentage of MHC-multimer-positive cells from all CD8+ T cells measured by flow cytometry is shown on a log-scale.

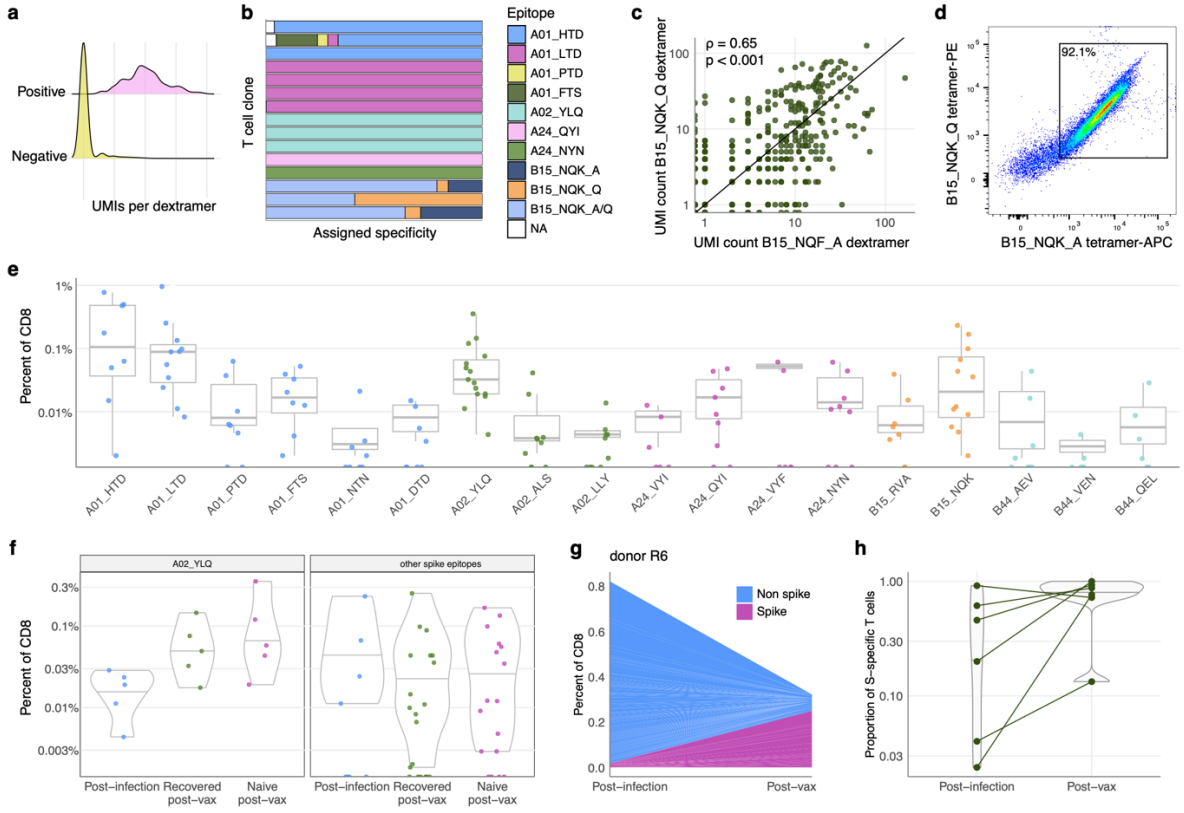


**Figure 2. Magnitude, dynamics, and cross-reactivity of CD8+ epitope-specific responses to SARS-CoV-2 infection and vaccination. a. Antigen specificity of each T cell could be inferred from dextramer-barcode UMI counts.** Representative distribution of the number of UMIs in cells called dextramer-positive (pink) and dextramer-negative (yellow). **b. T cells within a clone have consistent specificity assignments, except T cells that cross-react with common cold coronavirus epitopes (B15_NQK_A/B15_NQK_Q pair).** Each bar shows a fraction of cells of a given clonotype attributed to different dextramers. The 15 most abundant clones (more than 12 cells) are shown. **c. The same cells bind both SARS-CoV-2 and CCCoV variants of the HLA-B*15:01-restricted spike-derived (NQKLIANA|QF) epitope.** Number of UMIs for B15_NQK_Q (SARS-CoV-2) and B15_NQK_A (OC43 and HKU1) dextramers are correlated (Spearman $\rho$=0.65, $p<0.001$). **d. Cross-reactivity between HLA-B*15:01-NQK epitope variants confirmed *in vitro*.** Jurkat cell line expressing αβTCR identified from scTCRseq data binds pMHC multimers loaded with both SARS-CoV-2 and CCCoV variants of epitope. **e. A01_TTD, A01_LTD, A02_YLQ, B15_NQK epitopes elicit strongest T cell responses.** Each point is an estimated frequency of epitope-specific T cells in a sample. Estimated frequency was calculated as a fraction of dextramer-specific T cells in scRNAseq results multiplied by bulk frequency of dextramer-stained CD8+ cells of all CD8+ cells measured by flow cytometry. **f. Estimated frequency of spike-specific T cells are comparable between experimental groups** (right). A02_YLQ tends to elicit a stronger response in the context of vaccination (left). **g. Boosting of spike-specific epitope fraction after immunization (donor R6).** Each colored ribbon represents an estimated frequency of spike- (purple) or non-spike- (blue) specific T cell clones. **h. SARS-CoV-2 recovered individuals have a higher proportion of spike-specific T cells after vaccination than before vaccination.** The fraction of spike-specific T cells out of all epitope-specific T cells is plotted for paired post-infection and post-vaccination timepoints of COVID-19 recovered donors ($p$=0.047, Wilcoxon signed-rank test).

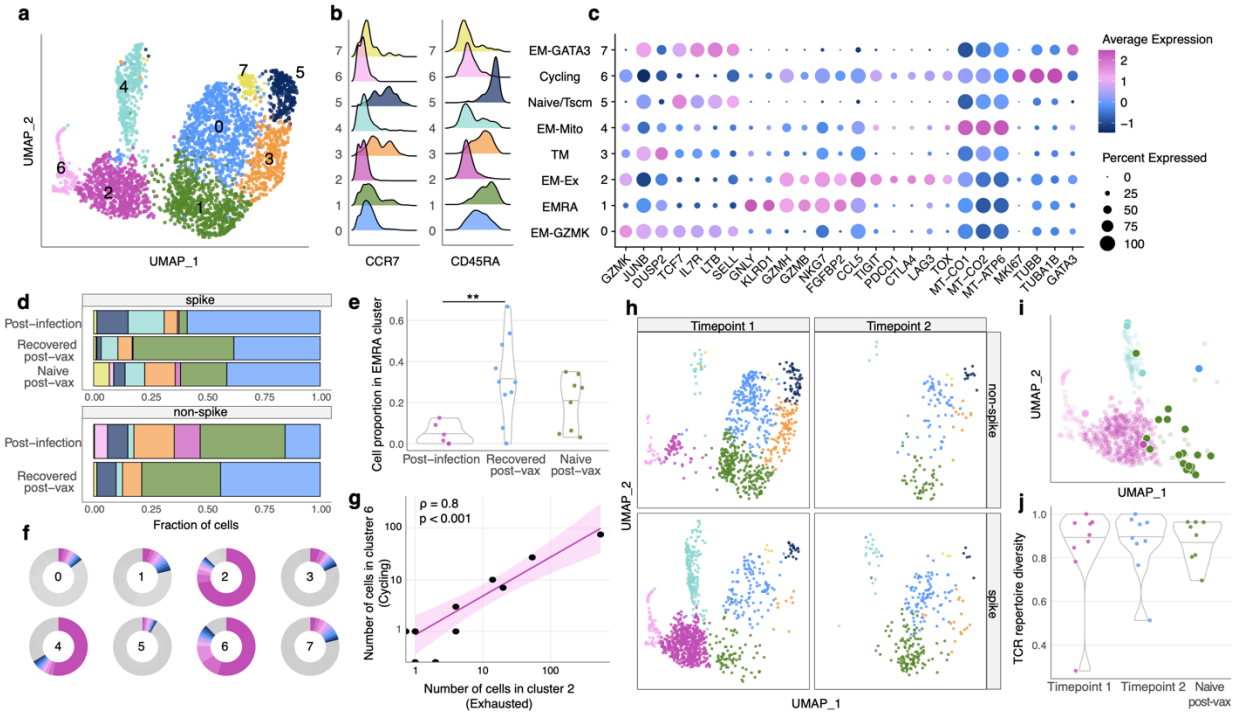


**Figure 3. Phenotypic diversity of epitope-specific CD8 T cells after natural SARS-CoV-2 infection and vaccination. a. UMAP (Uniform manifold approximation and projection) of all SARS-CoV-2 epitope-specific CD8 T cells based on gene expression (GEX).** Color shows results of graph-based unsupervised clustering performed with the Seurat package. **b. Density plot of CCR7 and CD45RA surface expression (measured by CITE-seq) in GEX clusters. c. Bubble plot of representative differentially expressed genes for each cluster.** Size of the circle shows percentage of cells in a cluster expressing a certain gene, color scale shows gene expression level. **d. Distribution of spike-specific (top subpanel) and non-spike-specific (bottom subpanel) T cells in gene expression clusters between study groups.** Colors show corresponding clusters from a, b. **e. Proportion of spike-specific T cells is significantly increased in EMRA cluster (cluster 1, green on d) after vaccination of SARS-CoV-2 recovered individuals, compared to the pre-vaccination timepoint (p=0.007, one-tailed Wilcoxon rank-sum test). f. Clone size distribution within GEX clusters.** Fractions of cells from 10 most abundant clonotypes in each cluster are shown with colors, all other clonotypes are shown in grey. Clusters 4, 6, and in particular 2 have the most expanded clones. **g. Number of cells in cluster 2 (Exhausted) and cluster 6 (Cycling) in samples are strongly correlated (Spearman ρ=0.8, p<0.001).** Shaded area shows 95% confidence interval for linear fit. **h. UMAP of spike-specific (bottom subpanel) and non-spike-specific (top subpanel) T cells sampled at two different timepoints from the same individuals based on GEX.** Cluster 2 of exhausted T cells and cluster 6 of cycling T cells disappear at the later timepoint irrespective of T cell specificity (spike or non-spike). **i. Distribution of cells from the largest observed clone between GEX clusters 7 days after the second dose (transparent dots) and 54 days after the second dose (opaque dots).** Although the vast majority of cells from exhausted cluster 2 (purple) disappear, the clone persists in memory subpopulations. **j. Vaccination of COVID-19 recovered does not affect spike-specific T cell repertoire diversity.** Normalized Shannon entropy of TCRβ is plotted for samples with more than 3 unique TCRβ clonotypes.

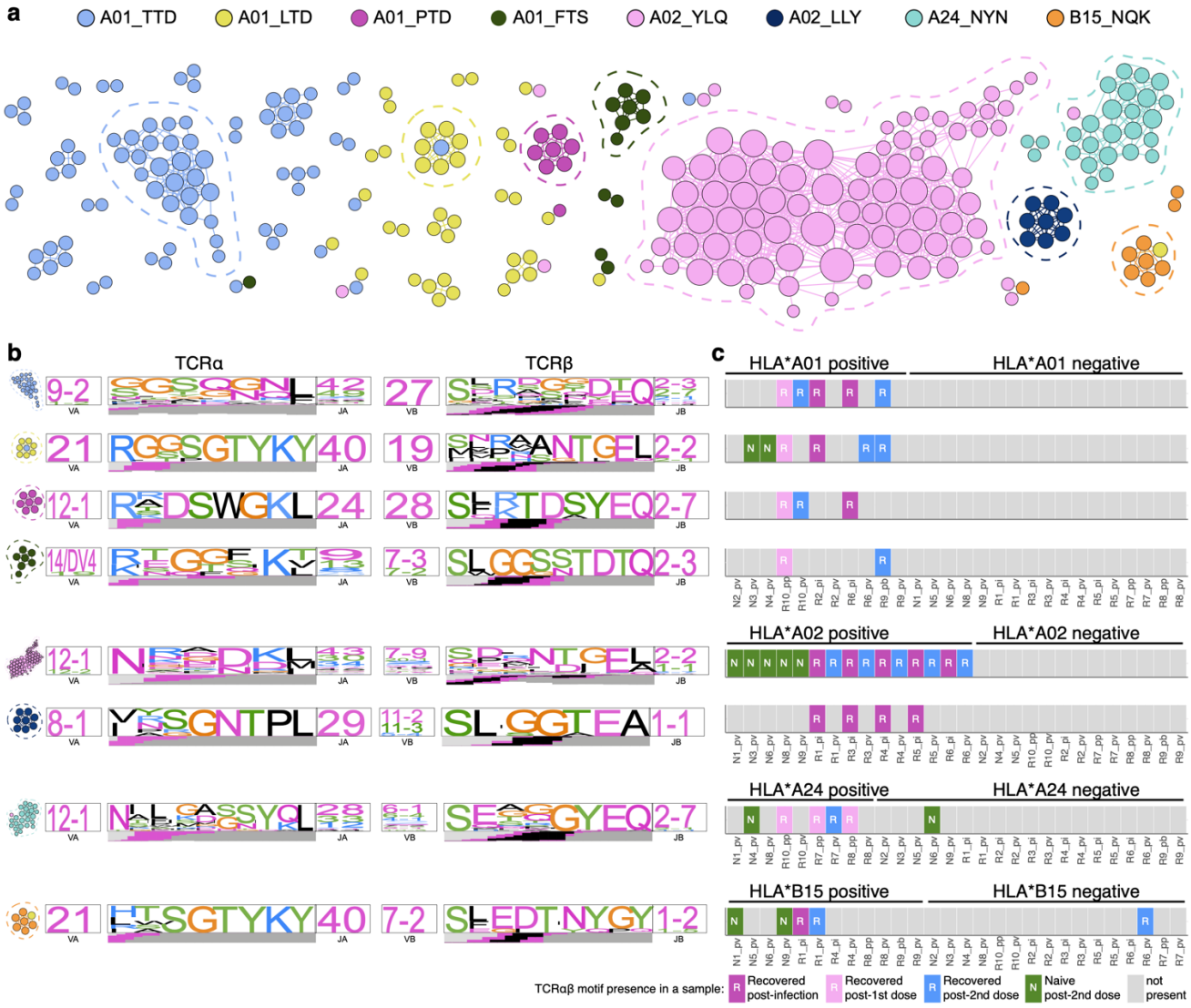


**Figure 4. Both SARS-CoV-2 infection and vaccination activate diverse polyclonal repertoire of epitope-specific T cells with distinctive sequence motifs. a. SARS-CoV-2 epitope-specific αβTCR amino acid clonotypes feature clusters of highly similar sequences with the same epitope specificity.** Each node on a similarity network is a unique paired αβTCR amino acid sequence, and an edge connects αβTCRs with TCRdist less than 120. Each color represents a certain epitope specificity. Clonotypes without neighbors are not shown. **b. TCR amino acid sequence motifs of α and β chains (TCRdist logos) for the largest clusters of highly similar TCRs for each epitope (circled with dashed line on A). c. TCRs with the same sequence motifs are found both after natural infection, and post-vaccination of both naive and recovered subjects in a matching HLA-background.** Occurrence of TCR motifs on the left is shown for all HLA matching and non-matching samples (rectangles on the plot). Grey rectangles represent samples lacking the TCR motif. The color of the rectangle that has a TCR motif corresponds to the sample group (purple for post-infection, pink, and blue for post-vaccination of recovered individuals, green for post-vaccination of naive individuals).

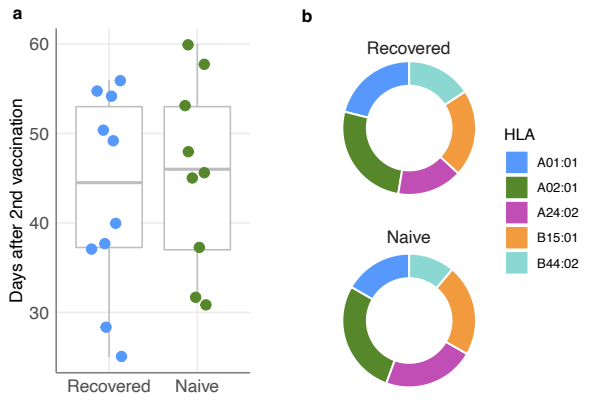


**Fig. S1. Subject selection for the study. a.** Time after second vaccination does not differ between recovered and immunologically naive groups. **b.** HLA-type distribution is similar across study groups.

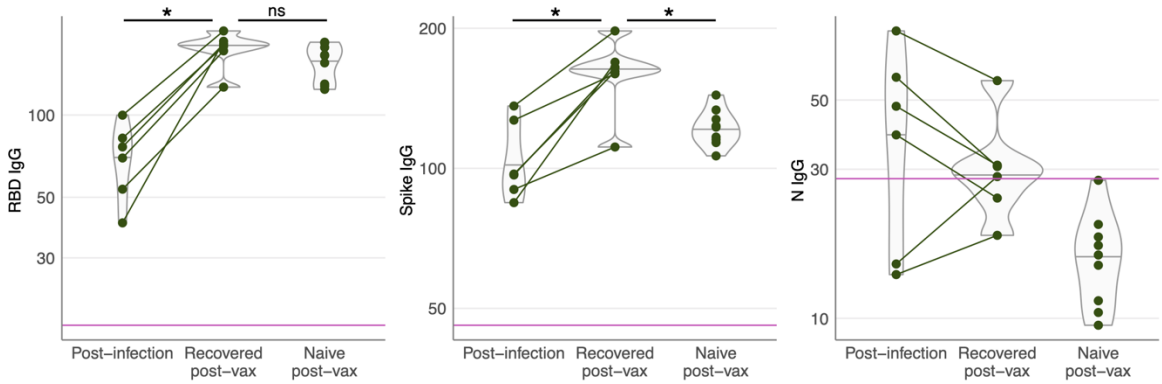


**Fig. S2. Antibody levels across study groups.** IgG levels to the receptor-binding domain (RBD) of the spike (left) and whole spike (middle) of SARS-CoV are boosted in recovered donors after vaccination (IgG RBD: p=0.016; IgG spike: p=0.016, Wilcoxon signed-rank test). Recovered donors after immunization have similar RBD IgG antibody levels (p=1, Wilcoxon rank-sum test), and even higher spike IgG (p=0.026, Wilcoxon rank-sum test) in comparison to SARS-CoV-2-naive vaccinated group. SARS-CoV-2 naive individuals are negative for N-specific IgG. Purple line on the plots indicates the positivity threshold.

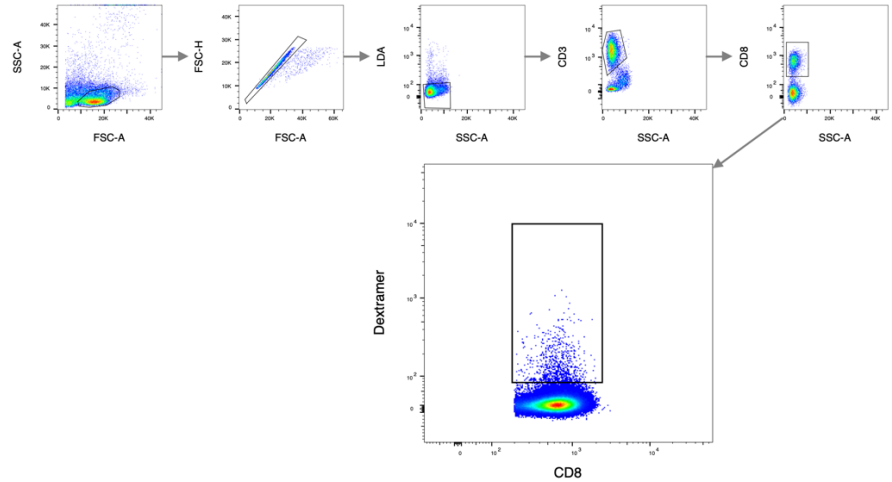


**Fig. S3. Gating strategy for sorting of single live CD3+CD8+dextramer+ cells.**

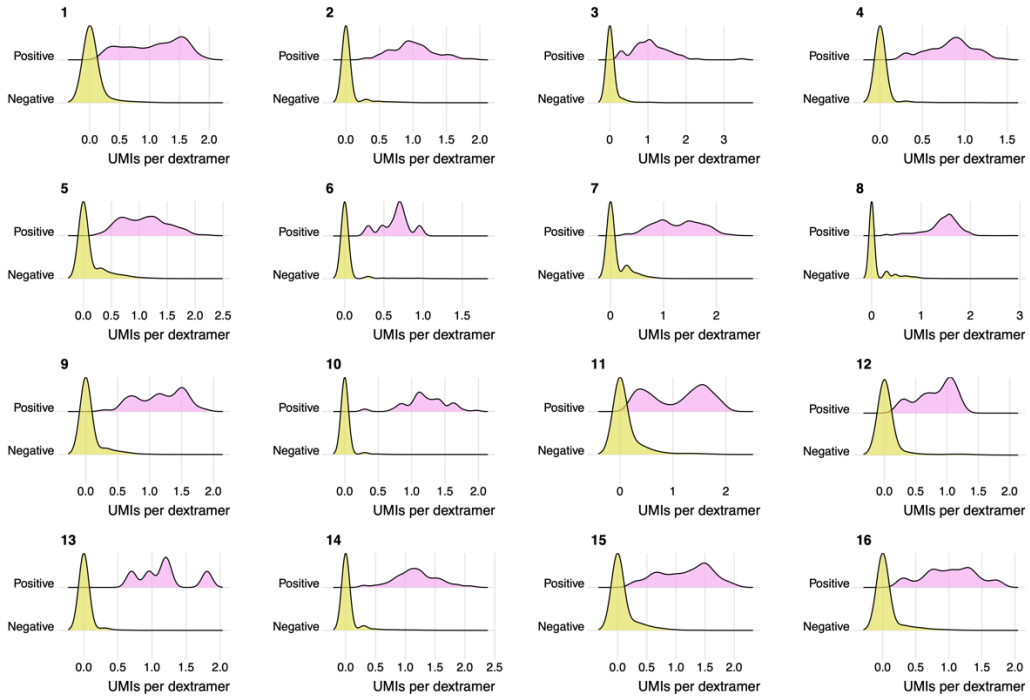


**Fig S4**. **Dextramer assignment with feature barcodes**. Each subplot shows distribution of $\mathrm{Log}_{10}$(# UMIs) for dextramers with certain feature barcodes in dextramer-negative (yellow) and dextramer-positive (pink) cells.

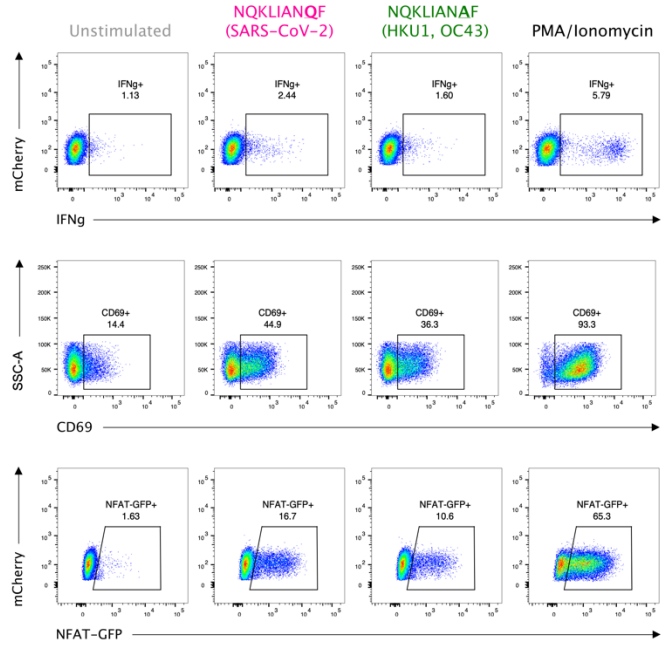


**Fig. S5**. **Peptide stimulation confirms cross-reactivity of B15_NQK αβTCR.** From left to right: unstimulated (negative control), NQKLIANQF (SARS-CoV-2) peptide stimulation, NQKLIANAF (OC43 and HKU1) peptide stimulation, PMA/Ionomycin (positive control). Top row: IFNgamma production by TCR-expressing Jurkats measured by intracellular cytokine staining. Middle row: CD69+ surface expression. Bottom row: NFAT-GFP reporter expression.

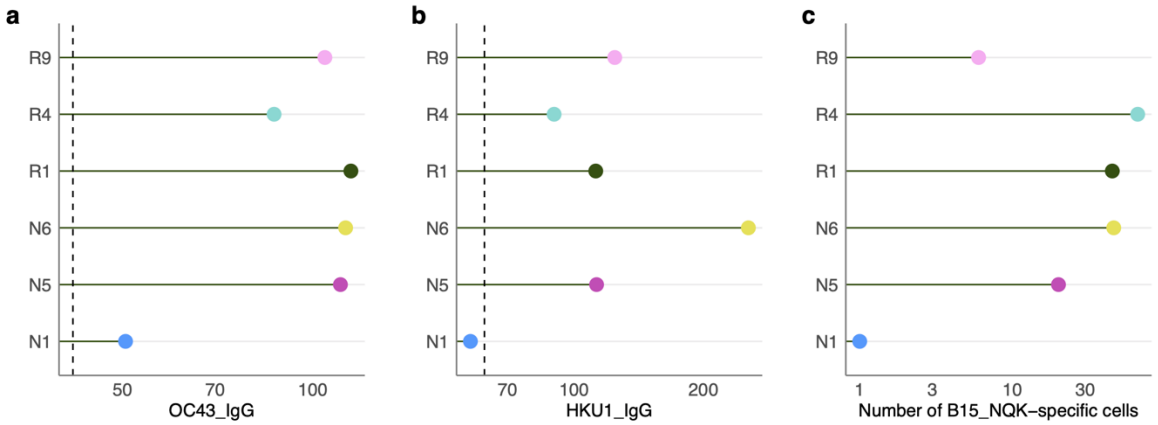


**Fig S6**. **Antibody titers for CCCoV spike protein (HKU1 left panel, OC43 middle panel) and number of B15-NQF/NAF cross-reactive cells in HLA*B15:01+ donors (right panel, log-scale).** Donor N1 has low levels of IgG anti-CCCoV antibodies and T cells cross-reactive with CCCoV derived HLA*B15:01-restricted epitope.

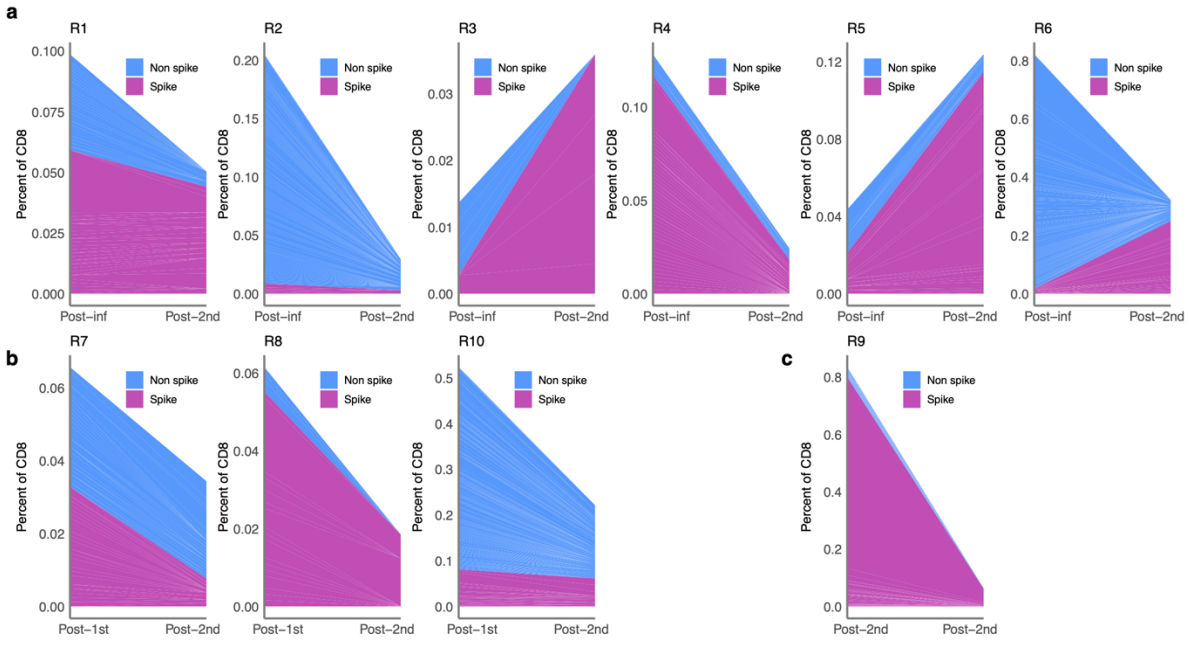


**Fig. S7. Clonal dynamics of spike and non-spike specific T cell response for each donor between two timepoints**. Each colored ribbon represents an estimated frequency of spike- (purple) or non-spike- (blue) specific T cell clones. **a.** Recovered donors (R1-R6), that have timepoint 1 sampled after the infection and timepoint 2 sampled after second dose of the vaccine. **b.** Recovered donors (R7, R8, R10), that have timepoint 1 sampled after the first dose of the vaccine and timepoint 2 sampled after the second dose of the vaccine. **c.** Recovered donor (R9), that have timepoint 1 sampled 7 days after the second dose of the vaccine and timepoint 2 sampled 54 days after second dose of the vaccine.

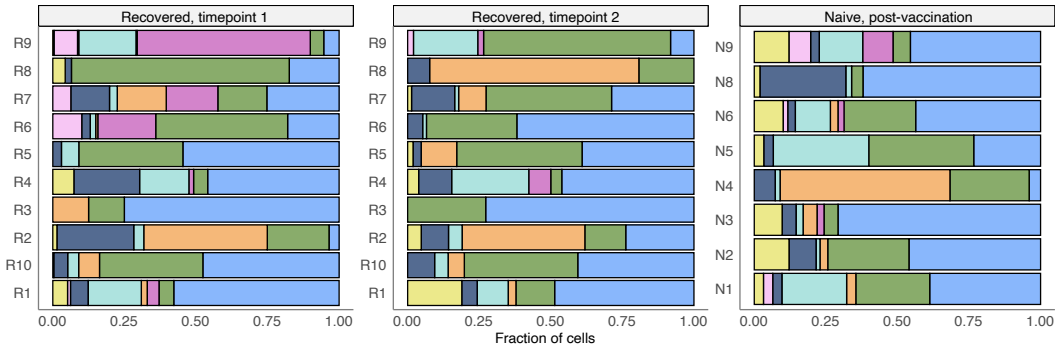


**Fig. S8. GEX cluster distribution for each sample**. Each coloured bar represents a fraction of cells in a given GEX cluster. See Fig. 3 a, b for UMAP and cluster identities (the colour code for clusters is consistent between figures).

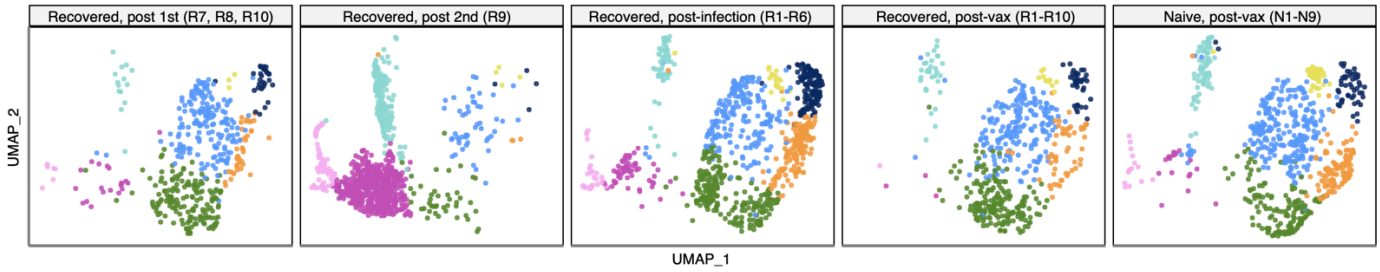


**Fig. S9. UMAP visualization of cells clustered by similarity of GEX**. Each subpanel shows cells from donors sampled at a given timepoint.

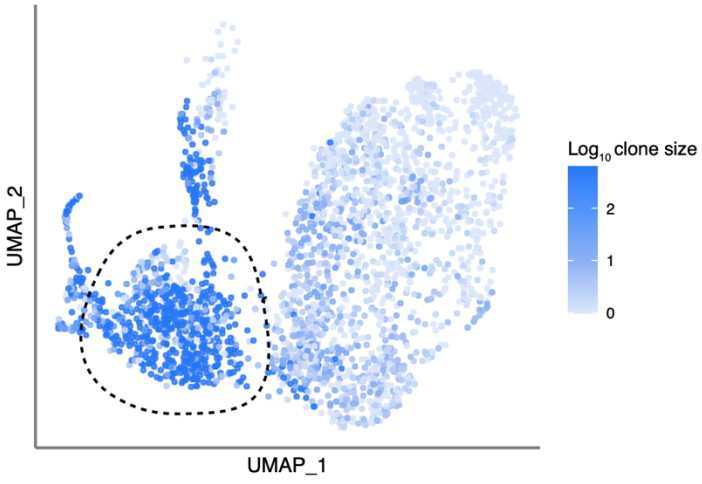


**Fig. S10. "Exhausted" cluster 2 (circled) is enriched with cells from expanded clones.** The color of each dot shows the size of the T cell clone ($Log_{10}$ of number of cells) for each cell.

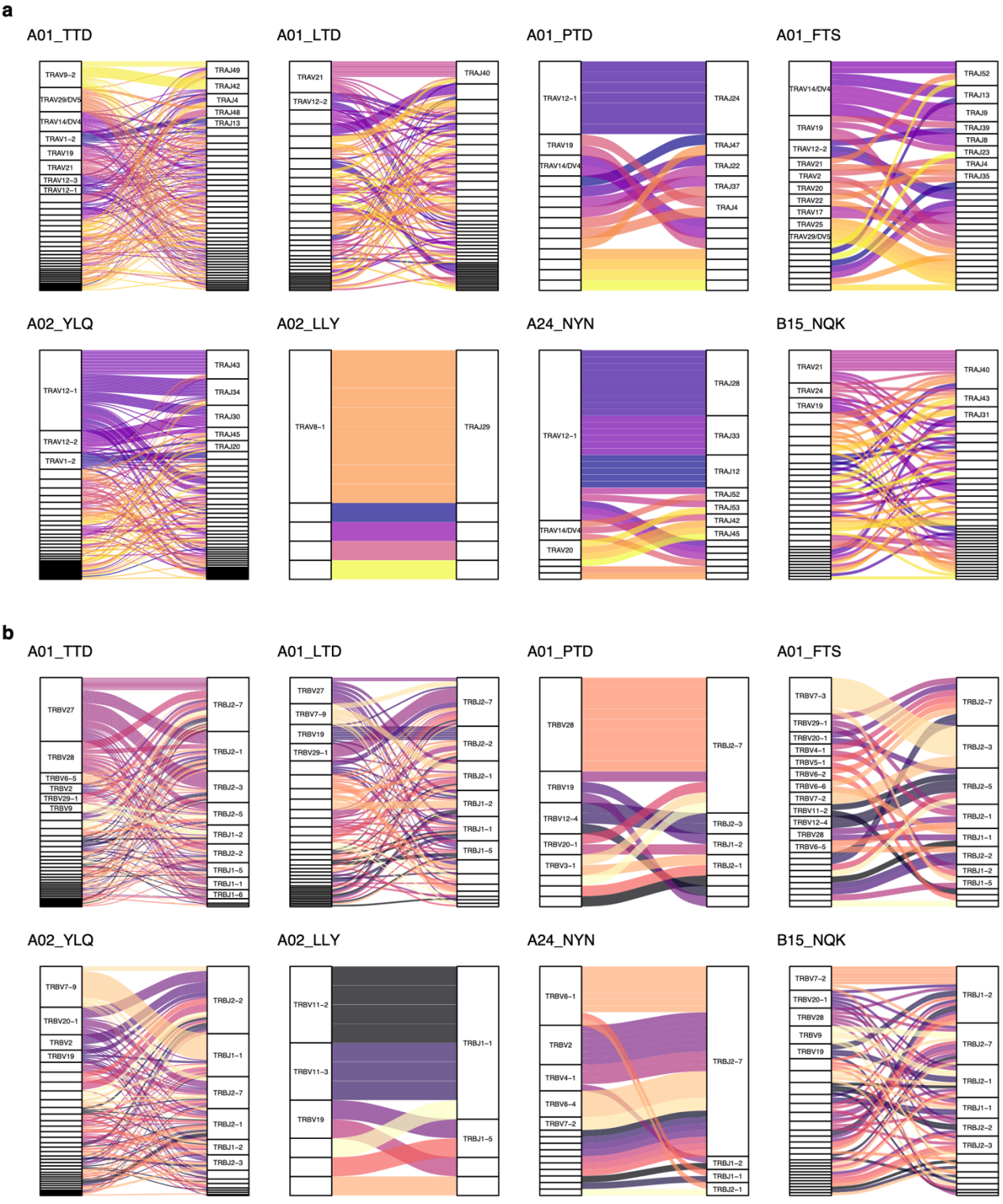


**Fig. S11. VJ-usage for immunodominant epitopes**. Height of each rectangle corresponds to the fraction of unique epitope-specific T cell clones expressing a given V- or J-segment in the TCRα **(a)** and TCRβ **(b)** chain. Ribbons show the frequency of VJ combinations.

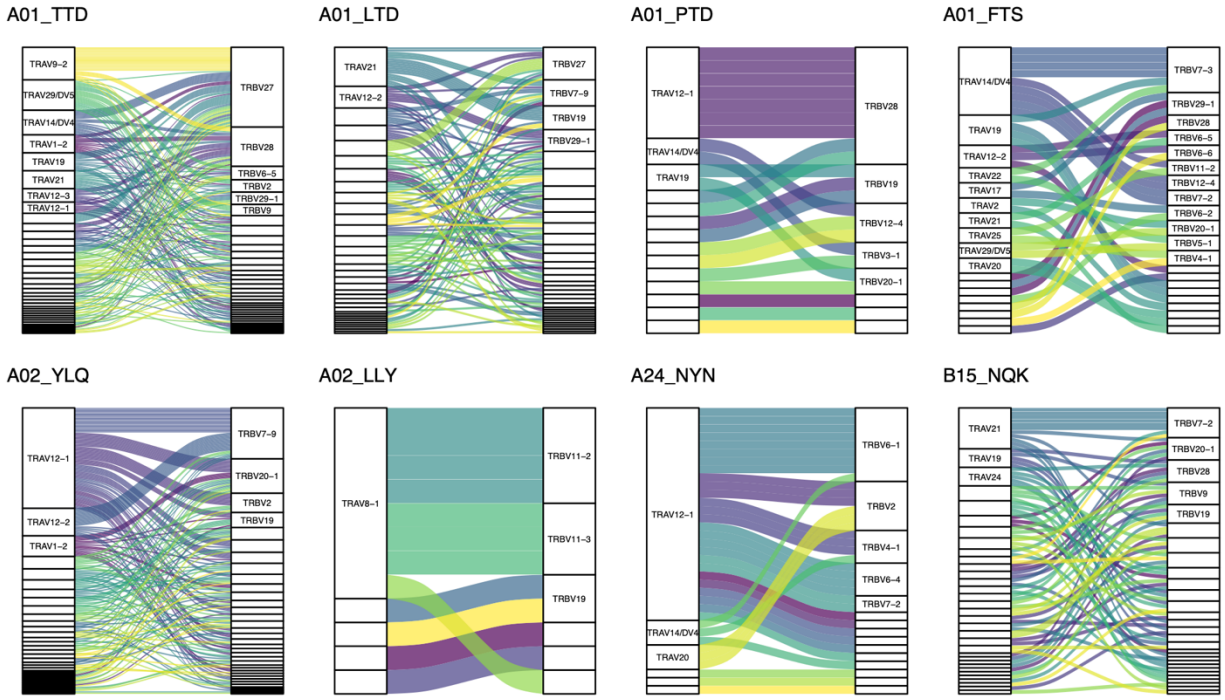


**Fig. S12. Vα-Vβ pairings for immunodominant epitopes.** Height of each rectangle corresponds to the fraction of unique epitope-specific T cell clones expressing a given TRAV or TRBV-segment. Ribbons show frequencies of TRAV-TRBV combinations.

## References

Amanat, Fatima, Daniel Stadlbauer, Shirin Strohmeier, Thi H. O. Nguyen, Veronika Chromikova, Meagan McMahon, Kaijun Jiang, et al. 2020. "A Serological Assay to Detect SARS-CoV-2 Seroconversion in Humans." *Nature Medicine* 26 (7): 1033–36. https://doi.org/10.1038/s41591-020-0913-5.

Camara, Carmen, Daniel Lozano-Ojalvo, Eduardo Lopez-Granados, Estela Paz-Artal, Marjorie Pion, Rafael Correa-Rocha, Alberto Ortiz, et al. 2021. "Differential Effects of the Second SARS-CoV-2 MRNA Vaccine Dose on T Cell Immunity in Naïve and COVID-19 Recovered Individuals." Preprint. Immunology. https://doi.org/10.1101/2021.03.22.436441.

Cornberg, Markus, Alex T. Chen, Lee A. Wilkinson, Michael A. Brehm, Sung-Kwon Kim, Claudia Calcagno, Dario Ghersi, et al. 2006. "Narrowed TCR Repertoire and Viral Escape as a Consequence of Heterologous Immunity." *The Journal of Clinical Investigation* 116 (5): 1443–56. https://doi.org/10.1172/JCI27804.

Csardi, Gabor, and Tamas Nepusz. 2006. "The Igraph Software Package for Complex Network Research." *InterJournal* Complex Systems: 1695.

Cukalac, Tania, Jesseka Chadderton, Andreas Handel, Peter C. Doherty, Stephen J. Turner, Paul G. Thomas, and Nicole L. La Gruta. 2014. "Reproducible Selection of High Avidity CD8+ T-Cell Clones Following Secondary Acute Virus Infection." *Proceedings of the National Academy of Sciences of the United States of America* 111 (4): 1485–90. https://doi.org/10.1073/pnas.1323736111.

Cukalac, Tania, Jessica M. Moffat, Vanessa Venturi, Miles P. Davenport, Peter C. Doherty, Stephen J. Turner, and John Stambas. 2009. "Narrowed TCR Diversity for Immunised Mice Challenged with Recombinant Influenza A-HIV Env(311-320) Virus." *Vaccine* 27 (48): 6755–61. https://doi.org/10.1016/j.vaccine.2009.08.079.

Dash, Pradyot, Andrew J. Fiore-Gartland, Tomer Hertz, George C. Wang, Shalini Sharma, Aisha Souquette, Jeremy Chase Crawford, et al. 2017. "Quantifiable Predictive Features Define Epitope-Specific T Cell Receptor Repertoires." *Nature* 547 (7661): 89–93. https://doi.org/10.1038/nature22383.

Diao, Bo, Chenhui Wang, Yingjun Tan, Xiewan Chen, Ying Liu, Lifen Ning, Li Chen, et al. 2020. "Reduction and Functional Exhaustion of T Cells in Patients With Coronavirus

Disease 2019 (COVID-19)." *Frontiers in Immunology* 11 (May): 827. https://doi.org/10.3389/fimmu.2020.00827.

Ebinger, Joseph E., Justyna Fert-Bober, Ignat Printsev, Min Wu, Nancy Sun, John C. Prostko, Edwin C. Frias, et al. 2021. "Antibody Responses to the BNT162b2 MRNA Vaccine in Individuals Previously Infected with SARS-CoV-2." *Nature Medicine* 27 (6): 981–84. https://doi.org/10.1038/s41591-021-01325-6.

Ferretti, Andrew P., Tomasz Kula, Yifan Wang, Dalena M.V. Nguyen, Adam Weinheimer, Garrett S. Dunlap, Qikai Xu, et al. 2020. "Unbiased Screens Show CD8+ T Cells of COVID-19 Patients Recognize Shared Epitopes in SARS-CoV-2 That Largely Reside Outside the Spike Protein." *Immunity* 53 (5): 1095-1107.e3. https://doi.org/10.1016/j.immuni.2020.10.006.

Francis, Joshua M., Del Leistritz-Edwards, Augustine Dunn, Christina Tarr, Jesse Lehman, Conor Dempsey, Andrew Hamel, et al. 2021. "Allelic Variation in Class I HLA Determines Pre-Existing Memory Responses to SARS-CoV-2 That Shape the CD8 $^{+}$ T Cell Repertoire upon Viral Exposure." Preprint. Immunology. https://doi.org/10.1101/2021.04.29.441258.

Gangaev, Anastasia, Steven L. C. Ketelaars, Olga I. Isaeva, Sanne Patiwael, Anna Dopler, Kelly Hoefakker, Sara De Biasi, et al. 2021. "Identification and Characterization of a SARS-CoV-2 Specific CD8+ T Cell Response with Immunodominant Features." *Nature Communications* 12 (1): 2593. https://doi.org/10.1038/s41467-021-22811-y.

Glanville, Jacob, Huang Huang, Allison Nau, Olivia Hatton, Lisa E. Wagar, Florian Rubelt, Xuhuai Ji, et al. 2017. "Identifying Specificity Groups in the T Cell Receptor Repertoire." *Nature* 547 (7661): 94–98. https://doi.org/10.1038/nature22976.

Goel, Rishi R., Sokratis A. Apostolidis, Mark M. Painter, Divij Mathew, Ajinkya Pattekar, Oliva Kuthuru, Sigrid Gouma, et al. 2021. "Distinct Antibody and Memory B Cell Responses in SARS-CoV-2 Naïve and Recovered Individuals Following MRNA Vaccination." *Science Immunology* 6 (58): eabi6950. https://doi.org/10.1126/sciimmunol.abi6950.

Habel, Jennifer R., Thi H. O. Nguyen, Carolien E. van de Sandt, Jennifer A. Juno, Priyanka Chaurasia, Kathleen Wragg, Marios Koutsakos, et al. 2020. "Suboptimal SARS-CoV-2−specific CD8 $^{+}$ T Cell Response Associated with the Prominent HLA-A*02:01 Phenotype." *Proceedings of the National Academy of Sciences* 117 (39): 24384–91.

https://doi.org/10.1073/pnas.2015486117.

Harris, Paul A., Robert Taylor, Brenda L. Minor, Veida Elliott, Michelle Fernandez, Lindsay O'Neal, Laura McLeod, et al. 2019. "The REDCap Consortium: Building an International Community of Software Platform Partners." *Journal of Biomedical Informatics* 95 (July): 103208. https://doi.org/10.1016/j.jbi.2019.103208.

Harris, Paul A., Robert Taylor, Robert Thielke, Jonathon Payne, Nathaniel Gonzalez, and Jose G. Conde. 2009. "Research Electronic Data Capture (REDCap)—A Metadata-Driven Methodology and Workflow Process for Providing Translational Research Informatics Support." *Journal of Biomedical Informatics* 42 (2): 377–81. https://doi.org/10.1016/j.jbi.2008.08.010.

Jacomy, Mathieu, Tommaso Venturini, Sebastien Heymann, and Mathieu Bastian. 2014. "ForceAtlas2, a Continuous Graph Layout Algorithm for Handy Network Visualization Designed for the Gephi Software." Edited by Mark R. Muldoon. *PLoS ONE* 9 (6): e98679. https://doi.org/10.1371/journal.pone.0098679.

Kared, Hassen, Andrew D. Redd, Evan M. Bloch, Tania S. Bonny, Hermi Sumatoh, Faris Kairi, Daniel Carbajo, et al. 2021. "SARS-CoV-2–Specific CD8+ T Cell Responses in Convalescent COVID-19 Individuals." *Journal of Clinical Investigation* 131 (5): e145476. https://doi.org/10.1172/JCI145476.

Krammer, Florian, Komal Srivastava, Hala Alshammary, Angela A. Amoako, Mahmoud H. Awawda, Katherine F. Beach, Maria C. Bermúdez-González, et al. 2021. "Antibody Responses in Seropositive Persons after a Single Dose of SARS-CoV-2 MRNA Vaccine." *New England Journal of Medicine* 384 (14): 1372–74. https://doi.org/10.1056/NEJMc2101667.

Kusnadi, Anthony, Ciro Ramírez-Suástegui, Vicente Fajardo, Serena J Chee, Benjamin J Meckiff, Hayley Simon, Emanuela Pelosi, et al. 2021. "Severely Ill COVID-19 Patients Display Impaired Exhaustion Features in SARS-CoV-2-Reactive CD8 $^{+}$ T Cells." *Science Immunology* 6 (55): eabe4782. https://doi.org/10.1126/sciimmunol.abe4782.

Malherbe, Laurent, Linda Mark, Nicolas Fazilleau, Louise J. McHeyzer-Williams, and Michael G. McHeyzer-Williams. 2008. "Vaccine Adjuvants Alter TCR-Based Selection Thresholds." *Immunity* 28 (5): 698–709. https://doi.org/10.1016/j.immuni.2008.03.014.

Mazzoni, Alessio, Nicoletta Di Lauria, Laura Maggi, Lorenzo Salvati, Anna Vanni, Manuela

Capone, Giulia Lamacchia, et al. 2021. "First-Dose MRNA Vaccination Is Sufficient to Reactivate Immunological Memory to SARS-CoV-2 in Subjects Who Have Recovered from COVID-19." *Journal of Clinical Investigation* 131 (12): e149150. https://doi.org/10.1172/JCI149150.

Minervina, Anastasia A, Ekaterina A Komech, Aleksei Titov, Meriem Bensouda Koraichi, Elisa Rosati, Ilgar Z Mamedov, Andre Franke, et al. 2021. "Longitudinal High-Throughput TCR Repertoire Profiling Reveals the Dynamics of T-Cell Memory Formation after Mild COVID-19 Infection." *ELife* 10 (January): e63502. https://doi.org/10.7554/eLife.63502.

Nelde, Annika, Tatjana Bilich, Jonas S. Heitmann, Yacine Maringer, Helmut R. Salih, Malte Roerden, Maren Lübke, et al. 2021. "SARS-CoV-2-Derived Peptides Define Heterologous and COVID-19-Induced T Cell Recognition." *Nature Immunology* 22 (1): 74–85. https://doi.org/10.1038/s41590-020-00808-x.

Nguyen, Thi H.O., Louise C. Rowntree, Jan Petersen, Brendon Y. Chua, Luca Hensen, Lukasz Kedzierski, Carolien E. van de Sandt, et al. 2021. "CD8+ T Cells Specific for an Immunodominant SARS-CoV-2 Nucleocapsid Epitope Display High Naive Precursor Frequency and TCR Promiscuity." *Immunity* 54 (5): 1066-1082.e5. https://doi.org/10.1016/j.immuni.2021.04.009.

Nielsen, Stine SF, Line K Vibholm, Ida Monrad, Rikke Olesen, Giacomo S Frattari, Marie H Pahus, Jesper F Højen, et al. 2021. "SARS-CoV-2 Elicits Robust Adaptive Immune Responses Regardless of Disease Severity." *EBioMedicine* 68 (June): 103410. https://doi.org/10.1016/j.ebiom.2021.103410.

Oberle, Susanne G., Layane Hanna-El-Daher, Vijaykumar Chennupati, Sarah Enouz, Stefanie Scherer, Martin Prlic, and Dietmar Zehn. 2016. "A Minimum Epitope Overlap between Infections Strongly Narrows the Emerging T Cell Repertoire." *Cell Reports* 17 (3): 627–35. https://doi.org/10.1016/j.celrep.2016.09.072.

Painter, Mark M., Divij Mathew, Rishi R. Goel, Sokratis A. Apostolidis, Ajinkya Pattekar, Oliva Kuthuru, Amy E. Baxter, et al. 2021. "Rapid Induction of Antigen-Specific CD4 $^{+}$ T Cells Guides Coordinated Humoral and Cellular Immune Responses to SARS-CoV-2 MRNA Vaccination." Preprint. Immunology. https://doi.org/10.1101/2021.04.21.440862.

Peng, Yanchun, Alexander J. Mentzer, Guihai Liu, Xuan Yao, Zixi Yin, Danning Dong, Wanwisa Dejnirattisai, et al. 2020. "Broad and Strong Memory CD4+ and CD8+ T Cells

Induced by SARS-CoV-2 in UK Convalescent Individuals Following COVID-19." *Nature Immunology* 21 (11): 1336–45. https://doi.org/10.1038/s41590-020-0782-6.

Petrie, Joshua G., and Arnold S. Monto. 2017. "Untangling the Effects of Prior Vaccination on Subsequent Influenza Vaccine Effectiveness." *The Journal of Infectious Diseases* 215 (6): 841–43. https://doi.org/10.1093/infdis/jix056.

Reynisson, Birkir, Bruno Alvarez, Sinu Paul, Bjoern Peters, and Morten Nielsen. 2020. "NetMHCpan-4.1 and NetMHCIIpan-4.0: Improved Predictions of MHC Antigen Presentation by Concurrent Motif Deconvolution and Integration of MS MHC Eluted Ligand Data." *Nucleic Acids Research* 48 (W1): W449–54. https://doi.org/10.1093/nar/gkaa379.

Rha, Min-Seok, Hye Won Jeong, Jae-Hoon Ko, Seong Jin Choi, In-Ho Seo, Jeong Seok Lee, Moa Sa, et al. 2021. "PD-1-Expressing SARS-CoV-2-Specific CD8+ T Cells Are Not Exhausted, but Functional in Patients with COVID-19." *Immunity* 54 (1): 44-52.e3. https://doi.org/10.1016/j.immuni.2020.12.002.

Robinson, James, Dominic J Barker, Xenia Georgiou, Michael A Cooper, Paul Flicek, and Steven G E Marsh. 2019. "IPD-IMGT/HLA Database." *Nucleic Acids Research*, October, gkz950. https://doi.org/10.1093/nar/gkz950.

Sahin, Ugur, Alexander Muik, Evelyna Derhovanessian, Isabel Vogler, Lena M. Kranz, Mathias Vormehr, Alina Baum, et al. 2020. "COVID-19 Vaccine BNT162b1 Elicits Human Antibody and TH1 T Cell Responses." *Nature* 586 (7830): 594–99. https://doi.org/10.1038/s41586-020-2814-7.

Sahin, Ugur, Alexander Muik, Isabel Vogler, Evelyna Derhovanessian, Lena M. Kranz, Mathias Vormehr, Jasmin Quandt, et al. 2021. "BNT162b2 Vaccine Induces Neutralizing Antibodies and Poly-Specific T Cells in Humans." *Nature*, May. https://doi.org/10.1038/s41586-021-03653-6.

Saini, Sunil Kumar, Ditte Stampe Hersby, Tripti Tamhane, Helle Rus Povlsen, Susana Patricia Amaya Hernandez, Morten Nielsen, Anne Ortved Gang, and Sine Reker Hadrup. 2021. "SARS-CoV-2 Genome-Wide T Cell Epitope Mapping Reveals Immunodominance and Substantial CD8 $^{+}$ T Cell Activation in COVID-19 Patients." *Science Immunology* 6 (58): eabf7550. https://doi.org/10.1126/sciimmunol.abf7550.

Schattgen, Stefan A., Kate Guion, Jeremy Chase Crawford, Aisha Souquette, Alvaro Martinez

Barrio, Michael J.T. Stubbington, Paul G. Thomas, and Philip Bradley. 2020. "Linking T Cell Receptor Sequence to Transcriptional Profiles with Clonotype Neighbor Graph Analysis (CoNGA)." Preprint. Immunology. https://doi.org/10.1101/2020.06.04.134536.

Schreibing, Felix, Monica Hannani, Fabio Ticconi, Eleanor Fewings, James S Nagai, Matthias Begemann, Christoph Kuppe, et al. 2021. "Dissecting CD8+ T Cell Pathology of Severe SARS-CoV-2 Infection by Single-Cell Epitope Mapping." Preprint. Immunology. https://doi.org/10.1101/2021.03.03.432690.

Schulien, Isabel, Janine Kemming, Valerie Oberhardt, Katharina Wild, Lea M. Seidel, Saskia Killmer, Sagar, et al. 2021. "Characterization of Pre-Existing and Induced SARS-CoV-2-Specific CD8+ T Cells." *Nature Medicine* 27 (1): 78–85. https://doi.org/10.1038/s41591-020-01143-2.

Sekine, Takuya, André Perez-Potti, Olga Rivera-Ballesteros, Kristoffer Strålin, Jean-Baptiste Gorin, Annika Olsson, Sian Llewellyn-Lacey, et al. 2020. "Robust T Cell Immunity in Convalescent Individuals with Asymptomatic or Mild COVID-19." *Cell* 183 (1): 158-168.e14. https://doi.org/10.1016/j.cell.2020.08.017.

Shomuradova, Alina S., Murad S. Vagida, Savely A. Sheetikov, Ksenia V. Zornikova, Dmitry Kiryukhin, Aleksei Titov, Iuliia O. Peshkova, et al. 2020. "SARS-CoV-2 Epitopes Are Recognized by a Public and Diverse Repertoire of Human T Cell Receptors." *Immunity* 53 (6): 1245-1257.e5. https://doi.org/10.1016/j.immuni.2020.11.004.

Snyder, Thomas M., Rachel M. Gittelman, Mark Klinger, Damon H. May, Edward J. Osborne, Ruth Taniguchi, H. Jabran Zahid, et al. 2020. "Magnitude and Dynamics of the T-Cell Response to SARS-CoV-2 Infection at Both Individual and Population Levels." Preprint. Infectious Diseases (except HIV/AIDS). https://doi.org/10.1101/2020.07.31.20165647.

Stuart, Tim, Andrew Butler, Paul Hoffman, Christoph Hafemeister, Efthymia Papalexi, William M. Mauck, Yuhan Hao, Marlon Stoeckius, Peter Smibert, and Rahul Satija. 2019. "Comprehensive Integration of Single-Cell Data." *Cell* 177 (7): 1888-1902.e21. https://doi.org/10.1016/j.cell.2019.05.031.

Tarke, Alison, John Sidney, Conner K. Kidd, Jennifer M. Dan, Sydney I. Ramirez, Esther Dawen Yu, Jose Mateus, et al. 2021. "Comprehensive Analysis of T Cell Immunodominance and Immunoprevalence of SARS-CoV-2 Epitopes in COVID-19 Cases." *Cell Reports Medicine* 2 (2): 100204. https://doi.org/10.1016/j.xcrm.2021.100204.

943 Thevarajan, Irani, Thi H. O. Nguyen, Marios Koutsakos, Julian Druce, Leon Caly, Carolien E.
944 van de Sandt, Xiaoxiao Jia, et al. 2020. “Breadth of Concomitant Immune Responses
945 Prior to Patient Recovery: A Case Report of Non-Severe COVID-19.” *Nature Medicine*
946 26 (4): 453–55. https://doi.org/10.1038/s41591-020-0819-2.
947 Thimme, Robert, Valerie Oberhardt, Hendrik Luxenburger, Janine Kemming, Isabel Schulien,
948 Kevin Ciminski, Sebastian Giese, et al. 2021. “Rapid and Stable Mobilization of Fully
949 Functional Spike-Specific CD8+ T Cells Preceding a Mature Humoral Response after
950 SARS-CoV-2 MRNA Vaccination.” Preprint. In Review. https://doi.org/10.21203/rs.3.rs-
951 505193/v1.
952 Wang, Zijun, Frauke Muecksch, Dennis Schaefer-Babajew, Shlomo Finkin, Charlotte Viant,
953 Christian Gaebler, Hans- Heinrich Hoffmann, et al. 2021. “Naturally Enhanced
954 Neutralizing Breadth against SARS-CoV-2 One Year after Infection.” *Nature*, June.
955 https://doi.org/10.1038/s41586-021-03696-9.
956 Zheng, Hong-Yi, Mi Zhang, Cui-Xian Yang, Nian Zhang, Xi-Cheng Wang, Xin-Ping Yang,
957 Xing-Qi Dong, and Yong-Tang Zheng. 2020. “Elevated Exhaustion Levels and Reduced
958 Functional Diversity of T Cells in Peripheral Blood May Predict Severe Progression in
959 COVID-19 Patients.” *Cellular & Molecular Immunology* 17 (5): 541–43.
960 https://doi.org/10.1038/s41423-020-0401-3.
961
962
963
964